Manuscript title:

The V-type H^+-ATPase is targeted in anti-diuretic hormone control of the Malpighian 'renal' tubules

Farwa Sajadi[1], María Fernanda Vergara-Martínez[1,2] and Jean-Paul V. Paluzzi[1]*

1. Department of Biology, York University, 4700 Keele Street, Toronto, Ontario, M3J 1P3, Canada.
2. Departamento de Biología Celular y Fisiología, Instituto de Investigaciones Biomédicas, Universidad Nacional Autónoma de México, Mexico City, Mexico.

*Corresponding author: Jean-Paul V. Paluzzi
Email: paluzzi@yorku.ca

Author Contributions: J.-P.P. and F.S. designed research; F.S. and M.F.V. performed research; F.S. and J.P.P. analyzed data; and J.-P.P. and F.S. wrote the manuscript.
Competing Interest Statement: The authors declare no competing interest.
Classification: Biological Sciences; Physiology
Keywords: excretory system, *Aedes aegypti*, mosquito, anti-diuresis, proton pump, disease vector

This PDF file includes:

Main Text
Figures 1 to 6; S1 to S7

Abstract

Like other insects, secretion by mosquito Malpighian tubules (MTs) is driven by the V-type H^+-ATPase (VA) localized in the apical membrane of principal cells. The anti-diuretic neurohormone CAPA inhibits secretion by MTs stimulated by select diuretic hormones; however, the cellular effectors of this inhibitory signaling cascade remain unclear. Herein, we demonstrate that the VA inhibitor bafilomycin selectively inhibits serotonin (5HT)- and calcitonin-related diuretic hormone (DH_{31})-stimulated secretion. VA activity increases in DH_{31}-treated MTs, whereas CAPA abolishes this increase through a NOS/cGMP/PKG signaling pathway. A critical feature of VA activation involves the reversible association of the cytosolic (V_1) and membrane (V_o) complexes. Indeed, higher V_1 protein abundance was found in membrane fractions of DH_{31}-treated MTs whereas CAPA significantly decreased V_1 abundance in membrane fractions while increasing it in cytosolic fractions. Immunolocalization of V_1 was observed strictly in the apical membrane of MTs treated with DH_{31} alone whereas immunoreactivity was dispersed following CAPA treatment. VA complexes colocalized apically in female MTs shortly after a blood-meal consistent with the peak and post-peak phases of diuresis. Comparatively, V_1 immunoreactivity in MTs was more dispersed and did not colocalize with the V_o complex in the apical membrane at 3 hours post blood-meal, representing a timepoint after the late phase of diuresis has concluded. Therefore, CAPA inhibition of MTs involves reducing VA activity and promotes complex dissociation hindering secretion. Collectively, these findings reveal a key target in hormone-mediated inhibition of MTs countering diuresis that provides a deeper understanding of this critical physiological process necessary for hydromineral balance.

Significance Statement

The V-type H^+ ATPase (VA), also known as the proton pump, provides the driving force for transepithelial ion and fluid secretion in insect Malpighian tubules (MTs). While studies have shown that diuretic stimulation activates various signaling pathways promoting increased VA activity, our understanding of anti-diuretic signaling and its potential regulation of the VA remains rudimentary. Here we show that a CAPA neuropeptide acts through the NOS/cGMP/PKG pathway to inhibit VA activity, supporting the notion that the anti-diuretic regulation is achieved by promoting dissociation of the VA complexes. These results demonstrate a critical role of VA inhibition and trafficking necessary for anti-diuretic signaling and advances our understanding of the complex neuroendocrine control of the MTs in this important human disease-vector mosquito.

Main Text

Introduction

Insect post-prandial diuresis is under rigorous control by neuroendocrine factors (1) acting on the Malpighian 'renal' tubules (MTs) to regulate primary urine production. In the yellow fever mosquito, *Aedes aegypti*, several diuretics have been identified that regulate urine production including serotonin (5HT), calcitonin-related diuretic hormone (DH_{31}), corticotropin-releasing factor-related diuretic hormone (DH_{44}) and leucokinin-related (LK) diuretic hormone (2–5). An anti-diuretic peptidergic neurohormone, CAPA, selectively inhibits DH_{31}- and 5HT-stimulated secretion of MTs (4, 6, 7). Insect CAPA

neuropeptides are produced in the central nervous system and are evolutionarily related to the vertebrate neuromedin U peptides (8). In *Drosophila melanogaster*, CAPA peptides have been shown to act through a conserved nitridergic signaling pathway to stimulate diuresis by MTs (9, 10); however, a few other studies have alluded to an anti-diuretic role (11, 12). In contrast, in both larval and adult *A. aegypti*, CAPA peptides inhibit fluid secretion through a signaling cascade involving the NOS/cGMP/PKG pathway (6, 7). Despite this, the anti-diuretic signaling mechanism and downstream cellular targets, such as the ion channels and transporters, remain elusive.

In insect MTs, including *A. aegypti*, the bafilomycin-sensitive V-type H^+ ATPase (VA), also known as the proton pump, functions as an electrogenic pump allowing the transport of protons from the cytoplasm to the tubule lumen, thus generating a cell-negative membrane voltage (13, 14). This membrane voltage can then drive secondary transport processes such as the cation/H^+ exchanger or anion/H^+ cotransporter (15, 16). Originally found in vacuolar membranes of animals and plants, the VA has since been found to be essential in cell function in both invertebrates and vertebrates (17). In insects, the VA is densely located in the apical brush border membrane of tubule principal cells (13, 18), which is rich in mitochondria and endoplasmic reticula, fueling the ATP-consuming proton pump (1, 19). Previous studies have shown VA localization within the apical membrane of principal cells along the entire length of the MTs (19), but absent in stellate cells that express relatively higher levels of the P-type Na^+/K^+ ATPase (NKA) (19). Due to stronger VA immunoreactivity observed in MTs (19), and greater ATPase activity by electrophysiological assays (13, 14), the VA is categorized as serving mainly, but not exclusively (20), stimulated transport mechanisms, whereas the NKA serves basic

98 cell housekeeping functions when MTs are undergoing low unstimulated rates of
99 secretion (13, 20, 21).

100 Stimulation of distinct diuretic hormone receptors can activate various signaling
101 pathways, including elevation of cyclic AMP (cAMP) levels which is known to increase
102 VA activity and assembly in insects (22). *In A. aegypti,* DH_{31}, identified as the mosquito
103 natriuretic peptide (23), selectively activates transepithelial secretion of Na^+ in the MTs,
104 using cAMP as a second messenger (1), and upregulating the VA function to stimulate
105 fluid secretion (24). Similarly, 5HT-stimulated diuresis is also thought to be mediated (at
106 least in part) through the cAMP second messenger pathway (25), activating protein
107 kinase A (PKA) to increase the transepithelial voltage of the basolateral membrane in
108 tubule principal cells (1, 26). In contrast, DH_{44} has been shown to initiate diuresis via the
109 paracellular and transcellular pathways, with higher nanomolar concentrations increasing
110 cAMP and Ca^{2+}, influencing both paracellular and transcellular transport, and lower
111 nanomolar concentrations acting through the paracellular pathway only, via intracellular
112 Ca^{2+} (27). Thus, due to its predominant role in fluid secretion, the VA could be a likely
113 target for both diuretic and anti-diuretic factors.

114 Eukaryotic V-ATPases are a multi-subunit protein composed of up to 14 different
115 polypeptides, which form two major structural complexes. The peripheral V_1 complex
116 (400-600 kDa), is invariably present in the cytoplasm and interacts with ATP, ADP, and
117 inorganic phosphate (28). The cytosolic V_1 complex consists of eight different subunits
118 (A-H): a globular headpiece with three alternating subunits A and B forming a hexamer
119 with nucleotide binding sites located at their interface, a central rotor stalk with single
120 copies of subunits D and F, and lastly, a peripheral stalk made up of subunits C, E, G, and

H (28). The B subunit, shown to have high sequence similarity amongst several species from fungi to mammals (29, 30), is a 56 kDa polypeptide, and is one of the two sites (along with subunit A) (31) in the V_1 complex that binds ATP. In contrast, the membrane-integrated V_o complex (150-350 kDa) mediates the transport of H^+ across the membrane (28) and is composed of at least six different subunits, which collectively function in the proton translocation pathway (13, 28). Although the proton channel of the VA can be blocked pharmacologically by the macrolide antibiotic, bafilomycin (32), there are two known intrinsic mechanisms for VA regulation: firstly, through oxidation of the cystine residue on the A subunit of the V_1 complex, thus preventing ATP hydrolysis; secondly, through reversible disassembly of the V_1 complex from the holoenzyme (13, 33). While the role and regulation of the VA by diuretic hormones in insect MTs has been studied (34–36), research examining anti-diuretic signaling mechanisms involving the VA remain in their infancy.

This study aimed to identify the cellular targets necessary for CAPA-mediated inhibition of fluid secretion by MTs stimulated by select diuretic factors in adult female *A. aegypti*. Our results provide evidence that CAPA neuropeptides inhibit fluid secretion by VA complex dissociation, thus hindering VA function and activity that is essential for driving rapid post-prandial diuresis.

Results

Bafilomycin inhibits DH_{31}- and 5HT-stimulated fluid secretion rate. To determine the appropriate concentration of bafilomycin to test on adult *A. aegypti* MTs, several doses were applied against DH_{31}-stimulated tubules (Fig. S1). Higher doses of bafilomycin (10^-

^{4} M and 10^{-5} M) resulted in significant inhibition of fluid secretion rate, with maximal inhibition leading to a five-fold decrease, observed with treatment of 10^{-5} M bafilomycin. Next, to determine whether inhibiting the VA would decrease fluid secretion rate stimulated by other diuretic hormones, including 5HT and DH_{44}, the effect of 10^{-5} M bafilomycin on adult tubules stimulated with these diuretics was tested (Fig. 1). Fluid secretion rates were measured over 30 min under control (stimulated) conditions, and then at 10-min intervals in the presence of bafilomycin. Treatment of MTs with 10^{-5} M bafilomycin against DH_{31} led to a decrease of fluid secretion over the treatment interval. Specifically, 30 min after treatment with bafilomycin, fluid secretion rate was significantly reduced by over two-fold to 0.438±0.041 nL min^{-1}, compared to DH_{31} alone, 0.941±0.077 nL min^{-1} (Fig. 1A). Similar results were seen with 5HT-stimulated MTs; however, a decrease in fluid secretion was observed 30 min post-bafilomycin, with a significant inhibition 40 min after treatment (0.522±0.072 nL min^{-1}, 5HT alone vs. 0.182±0.045 nL min^{-1}, 5HT + bafilomycin) (Fig. 1B). Distinct from DH_{31} and 5HT-stimulated tubules, DH_{44}-stimulated secretion was insensitive to bafilomycin treatment (Fig. 1C). To confirm whether *Aedae*CAPA-1 anti-diuresis is mediated by VA inhibition, adult female MTs were treated with either DH_{31} alone or in combination with *Aedae*CAPA-1, bafilomycin, or both (Fig. 1D). MTs treated with either *Aedae*CAPA-1 or bafilomycin resulted in a significant inhibition of DH_{31}-stimulated secretion, and similar inhibition was observed when both *Aedae*CAPA-1 and bafilomycin were applied together with no evidence of any additive inhibitory effects (Fig. 1D).

166 ***Aedae*CAPA-1 and bafilomycin alkalinizes secreted fluid in DH_{31}- and 5HT-**
167 **stimulated MTs.** The VA pumps protons from the cell into the tubule lumen thus
168 generating an electromotive potential (20, 31) and providing energy to drive the secretion
169 of cations via Na^+/H^+ and/or K^+/H^+ antiporters (13). An indirect way to measure whether
170 *Aedae*CAPA-1 and bafilomycin inhibits VA activity involves measuring the pH of the
171 secreted fluid from diuretic-stimulated MTs treated with *Aedae*CAPA-1 or bafilomycin
172 (Fig. 1E-G). In DH_{31}-stimulated MTs treated with *Aedae*CAPA-1, there was an
173 immediate significantly higher pH in the secreted fluid (7.479±0.030) at 40 min relative
174 to control, increasing up to 7.73±0.038 at 60 min (Fig. 1E). Similarly, pH levels in DH_{31}-
175 stimulated MTs treated with bafilomycin were significantly higher (7.66±0.064) relative
176 to control at 40 min, increasing up to 7.855±0.074 at 60 min. Comparable to DH_{31},
177 addition of *Aedae*CAPA-1 or bafilomycin, significantly increased the pH of secreted fluid
178 from 5HT-stimulated MTs to 7.75±0.061 and 7.82±0.083 respectively, at the 60 min
179 mark (Fig. 1F). In contrast, unlike the effects observed with DH_{31}- and 5HT-stimulated
180 MTs, *Aedae*CAPA-1 or bafilomycin did not alter the pH of the secreted fluid in DH_{44}-
181 stimulated MTs (Fig. 1G). The pH increased from 7.4 to 7.9 during the 30-min DH_{44}
182 incubation; however, pH did not change following the addition of *Aedae*CAPA-1 or
183 bafilomycin. Separately, we conducted measurements in unstimulated tubules to verify
184 pH in these small droplets did not drift over a time frame consistent with our above
185 experiments. Unstimulated MTs were allowed to secrete, and the droplets were isolated
186 and their pH was measured over the course of 60 min. Over this incubation period, no
187 change was observed in the pH of secreted droplets from unstimulated MTs (Fig. 1H),
188 upholding the notion that the alkalinization of secreted fluid observed following

189 *Aedae*CAPA-1 (or bafilomycin) treatment of DH_{31}- and 5HT-stimulated MTs is a result
190 of VA inhibition. Additionally, unstimulated MTs treated with either *Aedae*CAPA-1 or
191 bafilomycin resulted in no significant changes in either secretion rate (Fig. S2A) or pH
192 (Fig. S2B).
193
194 ***Aedae*CAPA-1 increases cGMP and decreases cAMP levels in DH_{31}-treated MTs.** To
195 further clarify the CAPA signaling pathway involving the second messengers, cGMP and
196 cAMP, we sought to determine changes in levels of these cyclic nucleotides in MTs
197 incubated in DH_{31} alone or combined with *Aedae*CAPA-1. Treatment of MTs with DH_{31}
198 alone had basal levels of cGMP, 10.91±0.109 $pmol^{-1}$/tubule, comparable to saline treated
199 MTs. Treatment of MTs with *Aedae*CAPA-1 resulted in a significant increase in cGMP
200 levels compared to DH_{31}- incubated tubules, increasing to 11.39±0.101 $pmol^{-1}$/tubule
201 (Fig. 1I). Similar results were observed with MTs treated with both DH_{31} + *Aedae*CAPA-
202 1, with significantly increased cGMP levels of 11.39±0.123 $pmol^{-1}$/tubule (Fig. 1I)
203 compared to MTs treated with DH_{31} alone. In contrast, treatment of MTs with DH_{31} alone
204 led to significantly higher levels of cAMP, 9.153±0.039 $pmol^{-1}$/tubule, while baseline
205 levels of this second messenger were observed in saline, DH_{31} + *Aedae*CAPA-1, and
206 *Aedae*CAPA-1 treated tubules (Fig. 1J). To further confirm the stimulatory role of cAMP
207 and inhibitory role of cGMP, tubules were treated with either cyclic nucleotide alone and
208 secretion rates were measured (Fig. 1K). Unstimulated fluid secretion rates were
209 measured over the first 30 min, and then at 10-min intervals with either cAMP or cGMP.
210 Treatment of MTs with 10^{-4} M cAMP led to a significant increase over the treatment
211 interval, with fluid secretion rates increasing to 0.615±0.096 nL min^{-1} at 60 min,

compared to 10^{-8} M cGMP (0.052±0.091 nL min^{-1}) and unstimulated (0.065±0.091 nL min^{-1}) (Fig. 1K). Finally, to establish whether these cyclic nucleotide second messengers elicit antagonistic control of the MTs in adult *A. aegypti*, tubules were treated initially with cAMP over the first 30 min and then cGMP was added in the presence of cAMP for a subsequent 30 min (Fig. 1L). Similarly, we also tested the opposite treatment regime where MTs were treated initially with cGMP and subsequently with cAMP added along with cGMP. Treatment of cAMP-stimulated MTs with 10^{-8} M cGMP led to a significant decrease (~4-fold) over the treatment interval, with secretion rates decreasing to 0.231±0.113 nL min^{-1} at 60 min, compared to 10^{-4} M cAMP alone (0.931±0.134 nL min^{-1}). In contrast, cGMP-incubated tubules treated with 10^{-4} M cAMP led to a significant increase (~10-fold) in secretion rate (0.537±0.072 nL min^{-1}) compared to MTs treated with 10^{-8} M cGMP alone (0.045±0.018 nL min^{-1}).

Parallel studies examining cAMP levels were measured in DH_{44}-incubated MTs. Treatment of MTs with DH_{44} alone had high levels of cAMP, 9.115±0.0.061 $pmol^{-1}$/tubule, compared to saline treated MTs, 8.709±0.081 $pmol^{-1}$/tubule (Fig. S3A). Levels of cAMP remained unchanged in tubules treated with both DH_{44} + *Aedae*CAPA-1, 8.954±0.108 $pmol^{-1}$/tubule. To further resolve the cAMP signaling pathway downstream of DH_{31} and DH_{44} stimulated diuresis, a PKA inhibitor (KT5720) was tested against diuretic-stimulated MTs. KT5720 abolished the stimulatory effect of DH_{31}, whereas secretion by DH_{44}-treated MTs remained unchanged (Fig. S3B).

_Aedae_CAPA-1 decreases VA activity in DH_{31}-stimulated MTs through the NOS/cGMP/PKG pathway. In *Aedes* MTs, 50-60% of the total ATPase activity can be

attributed to a bafilomycin- and nitrate-sensitive component that reflects the activity of the VA pump (13). The remaining ATPase activity may be due to nucleotide cyclases, protein kinases, myosin, DNA helicases, and other ATP-consuming processes such as the NKA (13). As such, to determine whether CAPA inhibits VA and/or NKA function, female diuretic-stimulated MTs were challenged with *Aedae*CAPA-1 to measure the resultant NKA and VA activity. As expected, given its role as the natriuretic diuretic hormone, adult female MTs treated with DH_{31} resulted in a significant (> two-fold) increase of VA activity, 0.0329±0.0007 µmoles ADP/µg protein/hour, compared to saline controls, 0.0151±0.0021 µmoles ADP/µg protein/hour (Fig. 2A). Importantly, MTs incubated with both DH_{31} and *Aedae*CAPA-1 had significantly lower VA activity, resulting in activity levels indistinguishable from saline controls. In contrast, neither 5HT nor DH_{44} influenced VA activity ($p>0.05$) when compared with saline controls, while co-treatment with *Aedae*CAPA-1 also resulted in indistinguishable VA activity. Similar VA activity levels were observed between 5HT and DH_{44} (0.0255±0.0078 and 0.0208±0.0042 µmoles ADP/µg protein/hour) and with co-application of *Aedae*CAPA-1 (0.0150±0.0036 and 0.0154±0.0070 µmoles ADP/µg protein/hour). Unlike changes observed in VA activity following treatment with DH_{31}, diuretic-stimulation or *Aedae*CAPA-1 treatment did not perturb NKA activity, with levels similar to that of unstimulated MTs (Fig. 2B).

To confirm the actions of CAPA are mediated through the NOS/cGMP/PKG pathway, pharmacological blockers, including inhibitors of NOS ($_L$-NAME) and PKG (KT5823), were tested against DH_{31}-stimulated MTs treated with either *Aedae*CAPA-1 or cGMP (Fig. 2C). Application of $_L$-NAME or KT5823 abolished the inhibitory effect of *Aedae*CAPA-1, resulting in high levels of VA activity, 0.02671±0.0025 and

0.03653±0.0051 µmoles ADP/µg protein/hour respectively, compared to MTs treated with DH_{31} + *Aedae*CAPA-1. As expected, treatment of DH_{31}-stimulated MTs with cGMP resulted in a significant decrease in VA activity, 0.006±0.0026 µmoles ADP/µg protein/hour, similar to *Aedae*CAPA-1-treated MTs, while co-treatment with KT5823, abolished the inhibitory effect of cGMP, resulting in an increase in VA activity.

***Aedae*CAPA-1 leads to VA holoenzyme dissociation in DH_{31}-treated MTs.** The reversible dissociation of the V_1 complex from the V_o membrane-integrated complex is a well-known mechanism for regulating VA transport activity (22, 31, 34, 35, 37). To determine whether *Aedae*CAPA-1 influences VA complex dissociation, membrane and cytosolic protein fractions were isolated from DH_{31} and DH_{31} + *Aedae*CAPA-1 incubated MTs, and a polyclonal V_1 antibody (13) was used to measure protein abundance. First, membrane and cytosolic protein isolation was verified with specific cytosolic (beta-actin) and membrane (AQP1) markers (Fig. S4). Western blot analysis revealed three protein bands, with calculated molecular masses of 74 kDa, 56 kDa, and 32 kDa (13, 38) (Fig. S5). The V_1 complex is composed of eight subunits (A-H), which includes the A (~74kDa) and B subunit (~56Da) that are arranged in a ring forming the globular headpiece for ATP binding and hydrolysis (31). Additionally, studies have suggested that subunit D (~32kDa) alongside subunit F constitute the central rotational stalk of the V_1 complex (17). There was no difference in abundance observed for the A subunit (74 kDa band) in either membrane or cytosolic fractions between saline and DH_{31} treatments whereas DH_{31} + *Aedae*CAPA-1 incubated MTs had increased A subunit (74 kDa band) protein abundance in cytosolic fractions compared to saline treatment (Fig. 3A) and

281 decreased abundance in the membrane fraction compared to MTs treated solely with
282 DH_{31} (Fig. 3B). Similarly, the V_1 complex B subunit abundance (56 kDa band) was
283 similar in all treatments within the cytosolic protein fraction (Fig. 3C) whereas DH_{31} +
284 *Aedae*CAPA-1 incubated MTs had significantly lower abundance in membrane fractions
285 compared to MTs treated with DH_{31} alone (Fig. 3D). Finally, there was no difference in
286 abundance of the V_1 complex subunit D (32 kDa band) between saline and DH_{31} treated
287 MTs in neither cytosolic or membrane fractions. However, as observed for the A and B
288 subunit bands (74 and 56 kDa band, respectively) DH_{31} + *Aedae*CAPA-1 incubated MTs
289 showed a significant increase in the D subunit in cytosolic fractions compared to saline
290 treated MTs (Fig. 3E) and a decrease in its abundance in membrane fraction compared to
291 MTs treated with DH_{31} alone (Fig. 3F). In summary, all three of the V1 complex
292 immunoreactive bands corresponding to subunits A, B and D (74, 56 and 32 kDa,
293 respectively) showed significantly higher abundance in cytosolic protein fractions and
294 lower abundance in membrane fractions in DH_{31} + *Aedae*CAPA-1 incubated MTs.

295 To visualize this potential endocrine-mediated reorganization of the VA
296 holoenzyme in this simple epithelium, we immunolocalized the membrane-integrated V_o
297 and cytosolic V_1 complex in the female *A. aegypti* MTs. Transverse sections of saline-
298 incubated (control) MTs demonstrated moderate enrichment of V_o (Fig. 4A, red), and V_1
299 (Fig 4B, green) complexes in the apical membrane of principal cells (Fig. 4C, S6A-D).
300 Comparatively, DH_{31}-incubated MTs revealed intense localization of the V_o (Fig. 4D,
301 red), and V_1 (Fig 4E, green) complexes within principal cells, where V_1 staining was
302 strictly co-localized with V_o staining on the apical membrane (Fig. 4F, Fig. S6E-H).
303 Interestingly, although V_o immunolocalization was restricted to the apical membrane, V_1

304 immunoreactivity was observed in both the apical membrane and cytosolic region in
305 DH_{31} + *Aedae*CAPA-1 co-treated MTs (Fig. 4G-I, Fig. S6I-T). Immunostaining was
306 absent in control preparations probed with only secondary antibodies (not shown)
307 confirming the specific detection of the VA complexes with each primary antibody.
308 To investigate this endocrine-mediated phenomenon *in vivo*, we immunolocalized
309 the membrane-integrated V_o and cytosolic V_1 complex in blood-fed females at different
310 time points. Whole body sections of non-blood-fed similarly aged females (control)
311 demonstrated moderate enrichment of both V_o (Fig. 5A, red), and V_1 (Fig. 4B, green) in
312 the MTs, with minimal co-localization (Fig. 5C), resembling saline-incubated MTs.
313 Interestingly, blood-fed female MTs revealed strong co-localization of the V_o and V_1
314 complexes at 10 min (Fig. 5D-F) and 30 min (Fig. 5G-I) post blood-meal, whereas V_1
315 immunoreactivity was more dispersed in both the apical membrane and cytosolic area in
316 MTs 3 hrs post blood-meal (Fig. 5J-L), comparable to non-blood-fed females.
317

318 **Discussion**

319 The MTs of the *Aedes* mosquito are the main organs responsible for the secretion
320 of water and solutes, thereby contributing towards hydromineral homeostasis of the
321 animal (39). Active ion transport in *A. aegypti* MTs is accomplished mainly by the V-
322 ATPases (VA) densely localized in the apical brush-border membrane of principal cells,
323 that energize the apical and basolateral membrane as well as the paracellular pathway,
324 allowing for transepithelial secretion of NaCl, KCl, and other solutes (40). In animal
325 cells, V-ATPase molecules in the plasma membrane, especially on the apical membrane
326 of epithelial cells, contribute to extracellular acidification or alkalization, intracellular pH

homeostasis, or energize the plasma membrane for secondary active transport (41, 42). In insect MTs, the VA plays a major role in fluid secretion, thus serving as a primary target for both diuretic and, as this study demonstrates, anti-diuretic hormonal regulation of the insect 'renal' tubules. Although the structure and function of the VA has been elucidated in some detail (13, 20, 22, 31, 43–45), the regulation of the proton pump remains unclear. Of the various regulatory mechanisms for VA activity, the most studied is the reversible dissociation of the cytosolic V_1 complex from the membrane-integrated V_o complex, first established in the midgut of the tobacco hornworm, *Manduca sexta* and yeast, *Saccharomyces cerevisiae* (44, 46). In this study, the activity and regulation of the VA was investigated under both diuretic and anti-diuretic hormone control of the adult female *A. aegypti* MTs. Notably, the current results advance our knowledge of the anti-diuretic control of the *A. aegypti* MTs, revealing a cellular mechanism for CAPA inhibition of the MTs by targeting the VA to block fluid secretion stimulated by select diuretic factors. This includes inhibition of the DH_{31}-related mosquito natriuretic peptide, which is critical for the post-haematophagy diuresis that eliminates excess water and sodium originating from the bloodmeal-derived plasma.

In insects, water excretion is tightly regulated to maintain homeostasis of ions and water (1, 47, 48). Female *A. aegypti* engorge a salt- and water-rich bloodmeal to obtain the necessary nutrients and proteins for their eggs (1), with about 40% of the ingested water eliminated in the first hour post feeding (49). The high rates of water excretion along with the high rates of primary urine production post bloodmeal suggest a highly coordinated and defined hormonal regulation of the signaling processes and downstream cellular targets for ion and water transport (50). In *Aedes* MTs, fluid secretion increases at

least three-fold after stimulation with mosquito natriuretic peptide (identified as DH_{31}), via cAMP as a second messenger (1), activating PKA, which subsequently activates V-ATPase-driven cation transport processes (22, 35, 38). Herein we show that DH_{31}-stimulated secretion is inhibited by bafilomycin, thought to block the proton channel of the VA (32). Moreover, the addition of either bafilomycin or *Aedae*CAPA-1 caused alkalization of the secreted fluid, indicating inhibition of the VA, which may lead to constrained entry of cations across the apical membrane through a proposed alkali cation/proton antiporter (15, 16). Thus, since bafilomycin inhibits DH_{31}-stimulated secretion, this supports the VA as a target in the inhibition of fluid secretion. Consequently, the driving force for ion movement and osmotically-obliged water is reduced, but select Na^+ channels and cotransporters remain unaffected in the presence of *Aedae*CAPA-1, as observed by the unchanged natriuretic effect of DH_{31} despite reduced secretion rates in response to *Aedae*CAPA-1 (4). Similar results were seen in 5HT-stimulated secretion, albeit a partial inhibition. An earlier study demonstrated that Ca^{2+}-mediated diuresis does not require the assembly and activation of the VA (37, 38). The cAMP effect on the VA is implemented by protein kinase A (PKA), with inhibitors of PKA abolishing hormone-induced assembly and activation of the VA (34). Although the endogenous 5HT receptor expressed within the *A. aegypti* MTs necessary for diuretic activity remains elusive, in the kissing bug, *Rhodnius prolixus*, both cAMP and Ca^{2+} have been shown to initiate diuresis in response to 5HT (51), which could explain the partial inhibitory response of *Aedae*CAPA-1 inhibition on 5HT-stimulated tubules as Ca^{2+}-mediated diuresis is independent of the VA (38). Notably, the anticipated 5HT type 2 receptor subtype expressed in the principal cells of the MTs is predicted to couple

373 through a Gq/11 signaling mechanism (52) and likely excludes the type 7 Gs-coupled
374 receptor localized to tracheolar cells associated with the MTs (53, 54) as well as the type
375 1 Gi-coupled receptor localized to principal cells in larval stage mosquitoes (55).
376 Interestingly, DH_{44}-mediated stimulation was observed to be independent of the
377 VA, as bafilomycin had no effect on the secretion rate or pH of the secreted fluid
378 following application of this CRF-related diuretic peptide. Previous studies have noted
379 that low nanomolar concentrations of a DH_{44}-related peptide were linked to the
380 stimulation of the paracellular pathway only (27), mediating this action through
381 intracellular Ca^{2+} as a second messenger (56). In contrast, high nanomolar concentrations
382 of a DH_{44}-related peptide were shown to influence both paracellular and transcellular
383 transport, increasing intracellular Ca^{2+} and cAMP (56). Although haemolymph
384 concentrations of diuretic peptides have yet to be determined in mosquitoes, DH_{31} is
385 immediately released into circulation post bloodmeal, stimulating rapid secretion of Na^+
386 and excess water (23, 49). In contrast, DH_{44}-stimulated diuresis in *A. aegypti* involves
387 non-selective transport Na^+ and K^+ cations (4), this supports a delayed release of this
388 diuretic hormone post-feeding to maintain production (albeit reduced) of primary urine
389 whilst conserving Na^+ ions.
390 In unstimulated adult female *Aedes* MTs isolated *in vitro*, the VA exhibits
391 variable rates of enzyme activity, consistent with highly variable rates of secretion, as
392 found also in various other insect species (26, 57, 58). The VA is the main energizer in
393 MTs as 60% of total ATPase activity can be linked to the VA (13), whereas the NKA,
394 with around 28% of ATPase activity, also plays a role in membrane energization,
395 denoting a more important role in the function of MTs than was previously assumed (19,

38–40). Here we show a significant two-fold increase in VA activity in MTs treated with DH_{31} compared to the unstimulated MTs, with no change in VA activity in 5HT and DH_{44}-treated MTs. Notably, *Aedae*CAPA-1 treatment blocked the DH_{31}-driven increase in VA activity, which corroborates the reduced fluid secretion rate and alkalization of the secreted fluid. Additionally, we sought to establish the importance of the NOS/cGMP/PKG pathway in the inhibitory actions of *Aedae*CAPA-1 on VA association. In stimulated MTs treated with *Aedae*CAPA-1 along with NOS inhibitor, $_L$-NAME, or PKG inhibitor, KT5823, the inhibitory activity of *Aedae*CAPA-1 and its second messenger cGMP was abolished, resulting in elevated VA activity as a result of DH_{31} treatment. The present study examined the effects of *Aedae*CAPA-1 on DH_{31}-stimulated VA activation for the first time in insects. Stimulation of DH_{31} causes an increase in cAMP production, which activates Na^+ channels and the $Na^+/K^+/2Cl^-$ cotransporter in the basolateral membrane (59) and up-regulates VA activity (as shown herein and previously) critical for increased fluid secretion (24). The DH_{31} receptor (*Aaeg*GPRCAL1) is expressed in a distal-proximal gradient in the MTs, with greater expression in principal cells where the VA in the apical membrane is highly expressed (19, 60). The co-localization of the DH_{31} receptor, VA, and cation exchangers (61–63) in the distal segment of the MTs, along with the CAPA receptor (6), collectively supports the major roles DH_{31} and CAPA play in post-prandial diuresis and anti-diuresis, respectively. In contrast to the marked changes in VA activity in response to diuretic and anti-diuretic hormones, NKA activity remained unchanged in response to treatments conducted herein. Further studies should examine the potential role of the NKA in diuretic and anti-diuretic processes.

The reversible dissociation of the V_1 and V_o complexes is currently thought as a universal regulatory mechanism of V-ATPases, appearing to be widely conserved from yeast to animal cells (13, 22, 35, 64). Although previously shown with cAMP (24), it remained unclear whether other second messengers (eg. Ca^{2+}, cGMP, and nitric oxide) affect the assembly/disassembly of the V_1V_o complexes in insect MTs. In this study, VA protein abundance in membrane and cytosolic fractions of MTs was confirmed by western blot analyses. The 56 kDa band represents the B subunit (29), while the 74 kDa and 32 kDa bands are suggested to be the A and D subunits, respectively, of the V_1 complex (36). The higher abundance of these V_1 complex protein subunits in the cytosolic fraction and lower abundance in membrane fraction in *Aedae*CAPA-1-treated MTs provides novel evidence of hormonally-regulated V_1 dissociation from the holoenzyme in *A. aegypti* MTs. This was further confirmed with V_1 staining found both in the apical membrane and cytosol of the MTs treated with DH_{31} and *Aedae*CAPA-1 in contrast to the strict co-localization of the V_1 and V_o complex in the apical membrane of MTs treated with DH_{31} alone. In unstimulated *A. aegypti* MTs, 40-73% of the V_1 subunits were found to be membrane associated, with reassembly of the V_1V_o complex observed upon stimulation with cAMP analogues (38). Although studies have revealed that hormonal regulation can activate the assembly of the holoenzyme, the signaling mechanisms achieving this control are unclear. In this study, the data provides evidence of VA assembly in DH_{31}-treated MTs, with V_1 complex protein subunit enrichment found in the membrane fractions, confirming the crucial role of the VA in DH_{31}-stimulated secretion. Studies in *A. aegypti* have demonstrated the involvement of PKA in the activation and assembly of the VA upon natriuretic hormone (i.e. DH_{31}) stimulation and

indicate the phosphorylation of the VA subunits by PKA in the MTs (38). These studies indicate a regulatory role of PKA in VA assembly and its activation that may be independent or in addition to phosphorylation (38). In line with these earlier observations, the current results indicate PKA is critical for DH_{31}-stimulated fluid secretion by MTs whereas DH_{44}-stimulated diuresis was found to be PKA-independent.

Together, these results indicate that *Aedae*CAPA-1 binding to its cognate receptor in principal cells of the MTs (6), targets the NOS/cGMP/PKG pathway (4, 6) to inhibit DH_{31}-mediated elevation of cAMP (23, 59), which blocks PKA-activated VA association and prevents protons from being pumped across the apical membrane, resulting in a more alkaline lumen. Our study provides novel evidence that the anti-diuretic activity of CAPA is mediated through the dissociation of the VA holoenzyme involving the removal of the V_1 complex from the apical membrane, hindering luminal flux of protons that in turn starves cation/H^+ exchange, which ultimately reduces fluid secretion (Fig. 6). In *R. prolixus* MTs, the physiological roles of cGMP and cAMP were examined (65) suggesting cGMP inhibits fluid secretion by activating a phosphodiesterase (PDE) that degrades cAMP elevated following 5HT and diuretic hormone stimulation of MTs. Indeed, the current results demonstrated the addition of cAMP reversed the inhibitory effects of cGMP, while the addition of cGMP reduced the stimulatory response of cAMP, supporting that these two cyclic nucleotides facilitate two opposing physiological roles in the MTs of adult *A. aegypti*. The data herein reveals cGMP levels increase in MTs treated with CAPA alone or in combination with DH_{31} while cAMP levels decrease in MTs treated with CAPA in combination with DH_{31} compared to tubules stimulated with DH_{31} alone, which upholds the roles of cAMP and cGMP in diuretic and anti-diuretic signaling

pathways, respecitively. Interestingly, mid-nanomolar concentrations of DH_{44} also led to increased levels of cAMP, with levels unchanging in response to *Aedae*CAPA-1, raising doubt regarding the involvement of a PDE. Treatment of a PKA inhibitor, KT5720, abolished DH_{31}-stimulated secretion but had no effect on DH_{44}-mediated stimulation. It is well established that the effects of cAMP are mediated by activation of cAMP-dependent protein kinase (PKA), a major cAMP target, followed by phosphorylation of target proteins (66). More recently, in *D. melanogaster* MTs, two distinct cAMP pathways have been elucidated to sustain fluid secretion; a PKA-dependent pathway, shown to regulate basal fluid secretion in principal cells; and a PKA-independent pathway, specifically a stimulatory principal EPAC (exchange proteins directly activated by cAMP) pathway, stimulating fluid secretion above basal levels (67). Future studies should examine the potential DH_{44}-stimulated PKA-independent pathway leading to secretion in *A. aegypti* MTs.

In summary, our study highlights a novel target in the anti-diuretic signaling pathway of adult female *A. aegypti* MTs, emphasizing the intricate and precise regulatory mechanism of anti-diuresis. Although a plethora studies have investigated the process of hydromineral balance in terrestrial insects from a diuretic perspective (1, 10, 23, 68–70), these current findings advance our understanding of anti-diuretic hormone control while providing further evidence of a previously elusive endocrine regulatory mechanism of the VA in mosquitoes (Fig. 6). Given that many terrestrial insects are recognized as agricultural pests or disease vectors, further investigating the complex regulation of their ionic and osmotic balance may aid in lessening their burden on human health and

prosperity through development of improved management strategies that, at least in part, impede their neuroendocrine control of hydromineral homeostasis.

Materials and Methods

Animal rearing

Eggs of *Aedes aegypti* (Liverpool strain) were collected from an established laboratory colony described previously (4, 71). All mosquitoes were raised under a 12:12 light:dark cycle. Non-blood fed female insects (three-six days post-eclosion) were used for bioassays, dissected under physiological saline (*Aedes* saline) adapted from (59) that contained (in $mmol^{-1}$): 150 NaCl, 25 HEPES, 3.4 KCl, 7.5 NaOH, 1.8 $NaHCO_3$, 1 $MgSO_4$, 1.7 $CaCl_2$, and 5 glucose, and titrated to pH 7.1.

MT fluid secretion assay

In order to determine fluid secretion rates, modified Ramsay assays were performed as described previously (4, 72). Female adults (3-6 day old) were dissected under physiological *Aedes* saline prepared as described above, and MTs were removed and placed in a Sylgard-lined Petri dish containing 20 µL bathing droplets (1:1 mixture of Schneider's Insect Medium (Sigma-Aldrich): *Aedes* saline, immersed in hydrated mineral oil to prevent evaporation. The proximal end of each tubule was wrapped around a Minutien pin to allow for fluid secretion measurements. To investigate the effects of second messengers, cAMP and cGMP, on fluid secretion rate, 10^{-4} M 8 bromo-cAMP (cAMP) (23, 65) and 10^{-8} M 8 bromo-cGMP (cGMP) (4) (Sigma-Aldrich, Oakville, ON, Canada) were used against unstimulated MTs. To test the effects of the pharmacological

510 blocker KT5720 (7) (protein kinase A (PKA) inhibitor), a dosage of 5 µmol l^{-1}
511 (manufacturer's recommended dose) was used against 25 nmol l^{-1} DH_{31}- and 10 nmol l^{-1}
512 DH_{44}-stimulated MTs.
513
514 **Time course inhibition of bafilomycin**
515 Dosage of bafilomycin A_1 was based on a dose-response analysis of bafilomycin
516 against DH_{31}-stimulated tubules (Fig. S1). In the interest of determining whether
517 bafilomycin inhibits the effects of the diuretic factors, dosages of 25 nmol l^{-1} *Drome*DH_{31}
518 (~84% identical to *Aedae*DH_{31}) (4, 23, 73), 100 nmol l^{-1} 5HT (4, 69, 74), and 10 nmol l^{-1}
519 *Rhopr*DH (CRF-related diuretic peptide, DH_{44}) (~48% overall identity; ~65% identity
520 and ~92% similarity within the highly-conserved N-terminal region to *Aedae*DH_{44}) (4,
521 56, 75, 76), were applied to the isolated MTs. Neurohormone receptors, including those
522 for 5HT, and the peptides DH_{31}, DH_{44}, and CAPA, are localized to the basolateral
523 membrane of principal cells (6, 61, 82), while the LK receptor is localized exclusively to
524 stellate cells (5). As a result, the effects of bafilomycin were tested on diuretics known to
525 act on the principal cells of the MTs. After incubating with the individual diuretics for 30
526 min (using the modified Ramsay assay), diuretic peptide was added alone (controls) or in
527 combination with bafilomycin (final concentration 10^{-5} M). The fluid secretion rate was
528 recorded every 10 min for a total of 80 min. In order to determine whether inhibition of
529 the VA was involved in the anti-diuretic activity of CAPA peptides on adult MTs, the
530 effects of 1 fmol l^{-1} *Aedae*CAPA-1 (4, 6) were investigated in combination with DH_{31}
531 and bafilomycin.
532

Measurement of pH of secreted fluid

The pH of secreted fluid was measured by using ion-selective microelectrodes (ISME) pulled from glass capillaries (TW-150-4, World Precision Instruments, Sarasota, Fl, USA) using a Sutter P-97 Flaming Brown pipette puller (Sutter Instruments, San Raffael, CA, USA). Microelectrodes were silanized with *N,N*-dimethyltrimethylsilylamine (Fluka, Buchs, Switzerland) pipetted onto the interior of a glass dish inverted over the group of microelectrodes. A 1:2 ratio of number of microelectrodes to amount of silanization solution (in µl) was used. The microelectrodes were left to silanize for 75 min at 350°C and left to cool before use. The microelectrodes were back-filled with a solution containing 100 mmol l^{-1} NaCl and 100 mmol l^{-1} sodium citrate that was titrated to pH 6.0 and front-filled using Hydrogen Ionophore I – cocktail B (Fluka, Buchs, Switzerland). The electrode tips were then coated with ~3.5% (w/v) polyvinyl chloride (PVC) dissolved in tetrahydrofuran, to avoid displacement of the ionophore cocktail when submerged in the paraffin oil (77). The H^+-selective microelectrodes were calibrated in *Aedes* saline titrated to either pH 7.0 or pH 8.0. Reference electrodes were prepared from glass capillaries (1B100F-4, World Precision Instruments) using a pipette puller described above and were backfilled with 500 mmol l^{-1} KCl. Secreted droplet pH measurements were done immediately after collection to prevent alkalization of the droplet due to carbon dioxide diffusion into the paraffin oil. Microelectrodes and reference electrodes were connected to an electrometer through silver chloride wires where voltage signals were recorded through a data acquisition system (Picolog for Windows, version 5.25.3). In order to measure pH of the secreted

fluid, tubules were set up using the Ramsay assay, and pH measurements were recorded every 10 min for a total of 60 min.

NKA and VA activities

The Na^+/K^+-ATPase (NKA) and VA activity in the MTs was determined using a modified 96-well microplate method (78, 79), which relies on the enzymatic coupling of ouabain- or bafilomycin-sensitive hydrolysis of ATP to the oxidation of reduced nicotinamide adenine dinucleotide (NADH). The microplate spectrophotometer is therefore able to directly measure the disappearance of NADH. Adult female MTs (three to six day old) were dissected and incubated for 30 min in *Aedes* saline, diuretic (DH_{31}, 5HT, or DH_{44}) alone or combined with *Aedae*CAPA-1. Following 30-min incubation, MTs were collected into 1.5 mL microcentrifuge tubes (40-50 sets of MTs per tube = 200-250 MTs per treatment), flash frozen in liquid nitrogen and stored at -80°C. To investigate the effects of the pharmacological blockers, a nitric oxide synthase (NOS) inhibitor, N_ω-Nitro-L-arginine methyl ester hydrochloride ($_L$-NAME), and protein kinase G (PKG) inhibitor, KT5823, were used against DH_{31}-stimulated MTs treated with *Aedae*CAPA-1 or 10^{-8} M cGMP. Dosages of 2 µmol l^{-1} $_L$-NAME (manufacturer's recommended dose) and 5 µmol l^{-1} KT582336 were applied to the MTs (4, 6, 7).

Tissues were thawed on ice and 150 µL of homogenizing buffer (four parts of SEI with composition (in mmol l^{-1}): 150 sucrose, 10 EDTA, and 50 imidazole; pH 7.3 and one part of SEID with composition: 0.5% of sodium deoxycholic acid in SEI) and MTs were then sonicated on ice for 10 sec (two pulses of 5 sec) and subsequently centrifuged

577 at 10,000 x *g* for 10 min at 4°C. The supernatant was transferred into a fresh
578 microcentrifuge tube and stored on ice.

579 Prior to the assay, three solutions were prepared (Solution A, B, and C) and all
580 stored on ice. Solution A contained 4 units mL^{-1} lactate dehydrogenase (LDH), 5 units
581 mL^{-1} pyruvate kinase (PK), 50 mmol l^{-1} imidazole, 2.8 mmol l^{-1} phosphoenolpyruvate
582 (PEP), 0.22 mmol l^{-1} ATP, and 50 mmol l^{-1} NADH, pH 7.5. The solution was
583 subsequently mixed with a salt solution in a 4:1 ratio (salt solution composition (in mmol
584 l^{-1}): 189 NaCl, 10.5 $MgCl_2$, 42 KCl, and 50 imidazole, pH 7.5. Working solution B
585 consisted of solution A with 5 mmol l^{-1} ouabain and solution C consisted of solution A
586 with 10 µmol l^{-1} bafilomycin. The concentrations of ouabain and bafilomycin were based
587 on previous studies (78). To ensure the batch of assay mixture (Solution A) was effective,
588 an adenosine diphosphate (ADP) standard curve was run. ADP standards were prepared
589 as follows: 0 nmol $10\mu L^{-1}$ (200µL of 50mmol l^{-1} imidazole buffer (IB), pH 7.5); 5 nmol
590 $10\mu L^{-1}$ (25µL of 4mmol l^{-1} ADP stock and 175µL of IB); 10 nmol $10uL^{-1}$ (50µL of
591 4mmol l^{-1} ADP stock/ 150 µL of IB); 20 nmol 10 μL^{-1} (100µL of 4mmol l^{-1} ADP
592 stock/100µL of IB); 40 nmol 10 μL^{-1} (40 mmol l^{-1} ADP stock). The standards were added
593 to a 96-well polystyrene microplate in duplicates of 10 µL per well, followed by the
594 addition of 200 µL of solution A. The plate was placed in a Thermo Multiscan Spectrum
595 microplate spectrophotometer set at 25°C and a linear rate of NADH disappearance was
596 measured at 340 nm. The absorbance spectra were recorded and analyzed using the
597 Multiscan Spectrum data acquisition system with SkanIt version 2.2 software. The ADP
598 standards (0 to 40 nmoles $well^{-1}$) should yield an optical density (OD) between 0.9 and
599 0.2 OD units, while the slope of the curve should result in -0.012 to -0.014 OD nmol

ADP^{-1}. Homogenized MT samples were thawed and added to the microplate (kept on ice) in six replicates of 10 µL per well. Next, two wells per sample were filled with 200 µL of working solution A, two wells with 200 µL of working solution B and two wells with 200 µL of working solution C (Fig. 4B). The microplate was quickly placed in the microplate spectrophotometer and the decrease in NADH absorbance was measured for 30 min at 340 nm. NKA and VA activity was calculated using the following equation:

$$\text{NKA or VA activity} = (((\Delta\text{ATPase}/S)/[P]) \times 60 \text{ (min)},$$

where ΔATPase is the difference in ATP hydrolysis in the absence and presence of ouabain or bafilomycin, *S* is the slope of the ADP standard curve, [P] is the protein concentration of the sample. Protein was quantified using a Bradford assay (Sigma-Aldrich Canada, Ltd.,) according to manufacturer's guidelines with bovine serum albumin (Bioshop Canada Inc., Burlington, ON, Canada) as a standard. Final activity was expressed as micromoles of ADP per milligram of protein per hour.

Protein processing and western blot analyses

MTs were isolated under physiological saline from 40-50 female *A. aegypti* for each biological replicate (defined as n = 1) and incubated for 60 min in the following three treatments: *Aedes* saline, 25 nmol l^{-1} DH_{31}, or 25 nmol l^{-1} DH_{31} + 1 fmol l^{-1} *Aedae*CAPA-1. Following the incubation, tissues were stored at -80ºC until processing. To separate the membrane and cytosolic proteins, a membrane protein extraction kit was used (ThermoFisher Scientific) following recommended guidelines for soft tissue with minor modifications including 200 µL of permeabilization and solubilization buffer and a 1:200 protease inhibitor cocktail (Sigma Aldrich) in both buffers. Final protein

623 concentrations were calculated by Bradford assay (Sigma-Aldrich Canada, Ltd.,)
624 according to manufacturer's guidelines with bovine serum albumin (BioRad
625 Laboratories) as a standard and quantified using an A_o Absorbance Microplate Reader
626 (Azure Biosystems) at 595 nm.

627 Protein samples were denatured by heating for 5 min at 100ºC with 6X loading
628 buffer (225 mmol l^{-1} Tris-HCl pH 6.8, 3.5% (w/v) SDS, 35% glycerol, 12.5% (v/v) ß-
629 mercaptoethanol and 0.01% (w/v) Bromophenol blue). Into each lane, 5 µg of protein
630 was loaded onto a 4% stacking and 12% resolving sodium dodecyl sulphate
631 polyacrylamide gel electrophoresis (SDS-PAGE) gel. Protein samples were migrated
632 initially at 80 V for 30 min and subsequently at 110 V for 90 min before being transferred
633 onto a polyvinylidene difluoride (PVDF) membrane using a wet transfer method at 100 V
634 for 60 min in a cold transfer buffer. Following transfer, PVDF membranes were blocked
635 with 5% skim milk powder in Tris-buffered saline (TBS-T; 9.9 mmol l^{-1} Tris, 0.15 mmol
636 l^{-1} NaCl, 0.1 mmol l^{-1} Tween-20, 0.1 mmol l^{-1} NP-40 pH 7.4) for 60 min at RT, and
637 incubated on a rocking platform overnight at 4ºC with a guinea pig polyclonal anti-VA
638 (Ab 353-2 against the V_1 complex of the VA (13), a kind gift from Profs. Wieczorek and
639 Tiburcy, University of Osnabruck, Germany, used at a 1:2000 dilution in 5% skim milk
640 in TBS-T. The next day, PVDF membranes were washed for 60 min in TBST-T,
641 changing the wash buffer every 15 min. Immunoblots were then incubated with a goat
642 anti-guinea pig HRP conjugated secondary antibody (1:2500 in 5% skim milk in TBS-T)
643 (Life Technologies, Burlington, ON) for 60 min at RT and subsequently washed three
644 times for 15 min with TBS-T. Lastly, blots were incubated with the Clarity Western ECL
645 substrate and images were acquired using a ChemiDoc MP Imaging System (Bio-Rad).

646 Molecular weight measurements were performed using Image Lab 5.0 software (Bio-
647 Rad). PVDF membranes were then probed with Coomassie brilliant blue, since total
648 protein normalization is now considered the benchmark method for quantitative analysis
649 of western blot data (80, 81) and has been used in studies involving *A. aegypti* protein
650 normalization (82). ImageJ software (NIH, USA) was used to quantify protein
651 abundance. (Fig. 3 and S5 show a saturated blot of the 56kDa band to ensure
652 visualization of the 74kDa and 32kDa band, however protein quantification was
653 measured using a pre-saturated blot).

654 To confirm successful separation of membranes from cytosol using the membrane
655 protein extraction kit, saline-incubated MTs were incubated in either anti-beta-tubulin
656 (cytosolic marker, 1:5000) or -AaAQP1 affinity purified rabbit polyclonal antibody
657 (generous gift from Dr. Andrew Donini, York University, Canada) (83) (membrane
658 marker, 1:1000). Blots were then incubated with a goat anti-mouse (for beta-tubulin) or
659 goat anti-rabbit (for AQP1) HRP-conjugated secondary antibody (1:5000 in 5% skim
660 milk in TBS-T) (Life Technologies, Burlington, ON) for 60 min at RT (beta-tubulin).
661

662 **Immunolocalization of VA complexes in MTs**

663 Immunohistochemistry of the MTs localizing the VA complexes was conducted
664 following a previously published protocol (84). Adult female MTs (three to six day old)
665 were dissected out in *Aedes* saline and incubated following similar conditions described
666 in the western blot section above. After the incubation, the MTs were immersed in
667 Bouin's solution and fixed for two hours in small glass vials. To test *in vivo* changes of
668 the VA complexes, five to six day old females were allowed to blood-feed for 20 min

669 (71), after which female mosquitoes were isolated at 10 min, 30 min, and 3 hr post blood-
670 meal. Similarly aged, non blood-fed (sucrose-fed) females were isolated as controls.
671 Following the bloodmeal, whole body females were immersed in Bouin's solution and
672 fixed for three hours in small glass vials. Tissues/whole body females were then rinsed
673 three times and stored in 70% ethanol at 4ºC until further processing. Fixed samples were
674 dehydrated through a series of ethanol washes: 70% ethanol for 30 min, 95% ethanol for
675 30 min, and 100% ethanol three times for 30 min. The samples were cleared with xylene
676 (ethanol:xylene for 30 min then 100% xylene three times for 30 min), and infiltrated in
677 Paraplast Plus Tissue Embedding Medium (Oxford Worldwide, LLC, Memphis, USA) at
678 xylene:paraffin wax for 60 min at 60ºC, then rinsed in pure paraffin wax twice for 1 hour
679 for 60ºC. Following the last rinse, the samples were embedded in the paraffin wax and
680 left to solidify at 4ºC until further processing. Sections (5 µm) were cut using a Leica RM
681 2125RT manual rotary microtome (Leica Microsystems Inc., Richmond Hill, Canada)
682 and slides were incubated overnight on a slide warmer at 45ºC.
683 The following day, sections were deparaffinized with xylene (two rinses for 5 min
684 each), and rehydrated via a descending series of ethanol washes (100% ethanol twice for
685 2 min, 95% ethanol for 2 min, 70% ethanol for 2 min, 50% ethanol for 2 min) and finally
686 in distilled water for 20 min. Next, sections were subjected to a heat-induced epitope
687 retrieval (HIER) by immersing slides in a sodium citrate buffer (10 nmol l^{-1}, pH 6.0) and
688 heating both slides and solution in a microwave oven for 4 min. The solution and slides
689 were allowed to cool for 20 min, reheated for 2 min, and left to stand at room temperature
690 (RT) for 15 min. Slides were then washed three times in phosphate-buffered saline (PBS)
691 pH 7.4, 0.4% Kodak Photo-Flo 200 in PBS (PBS/PF, 10 min), 0.05% Triton X-100 in

692 PBS (PBS/TX, 10 min), and 10% antibody dilution buffer (ADB; 10% goat serum, 3%
693 BSA and 0. 05% Triton X-100 in PBS) in PBS (PBS/ADB, 10 min). Slides were
694 incubated overnight at RT with a guinea pig polyclonal anti-V_1 (Ab 353-2 against the V_1
695 complex, identical antibody used in western blot analyses, at 1:5000 dilution in ADB) in
696 combination with a 1:100 mouse polyclonal anti-ATP6V0A1 antibody for V_o (Abnova,
697 Taipei, Taiwan).
698 Following overnight primary antibody incubation, slides were washed briefly in
699 distilled water, with sequential washes with PBS/PF, PBS/TX, and PBS/ADB for 10 min
700 each as described above. A goat anti-guinea pig antibody (for V_1 detection) conjugated to
701 AlexaFluor 488 (1:500 in ADB, Jackson Immunoresearch) and sheep anti-mouse
702 antibody (for V_0 detection) conjugated to AlexaFluor 594 (1:500 in ADB, Jackson
703 Immunoresearch) were applied to visualize the VA complexes. The slides were left to
704 incubate in the secondary antibody for 60 min at RT. For negative controls, slides were
705 processed as described above with primary antibodies omitted. Slides were then washed
706 in distilled water/0.4% PF three times for 1 min each and finally in distilled water for 1
707 min. Slides were air dried for 30 min and mounted using ProLong™ Gold antifade
708 reagent with DAPI (Life Technologies, Burlington, ON, Canada). Fluorescence images
709 were captured using an Olympus IX81 inverted fluorescent microscope (Olympus
710 Canada, Richmond Hill, ON, Canada).
711
712 **cGMP and cAMP Measurements**
713 A competitive cGMP ELISA kit (Cell Signaling Technology, #4360) and cAMP
714 ELISA kit (Cell Signaling Technology, #4339) were used to measure the effect of DH_{31},

715 DH_{44} and *Aedae*CAPA-1 on cGMP and cAMP levels in the MTs. Adult MTs were
716 isolated under physiological saline from 50 female *A. aegypti* for each biological
717 replicate (defined as n = 1). To prevent cGMP degradation, tubules were incubated first
718 with a phosphodiesterase inhibitor, 0.1 mmol l^{-1} zaprinast, for 10 min (85) or 0.5 mmol l^{-1}
719 3-isobutyl-1-methylxanthine (IBMX) for 10 min (23) before any of the experimental
720 treatments, specifically *Aedes* saline, 25 $nmol^{-1}$ DH_{31}, 10 nmol l^{-1} DH_{44}, 1 $fmol^{-1}$
721 *Aedae*CAPA-1, 25 $nmol^{-1}$ DH_{31} + 1 $fmol^{-1}$ *Aedae*CAPA-1, or 10 $nmol^{-1}$ DH_{44} + 1 $fmol^{-1}$
722 *Aedae*CAPA-1 for a further 20 min. After incubation was complete, tissues were stored at
723 -80ºC until processing. To measure cGMP and cAMP concentrations, frozen tubule
724 samples were thawed on ice and 125 µL of 1X cell lysis buffer (CLB, #9803) was added
725 to each tube (1 $mmol^{-1}$ phenylmethylsulfonyl fluoride (PMSF) was added to 1X CLB
726 fresh each time). Tissue samples were kept on ice for 10 min, sonicated for 10 s (similar
727 conditions as described for NKA/VA activity assay), centrifuged for 3 min at 10,000 rpm,
728 and the supernatant was isolated and kept on ice. Using a commercial 96-well microtitre
729 plate precoated with either a cGMP or cAMP rabbit monoclonal antibody, the cGMP-
730 HRP (or cAMP-HRP) conjugate was added in triplicate wells with 50 µL per well. This
731 was followed by the addition of 50 µL of either tubule samples or cGMP (or cAMP)
732 standards ranging from 100 $nmol^{-1}$ to 0.25 $nmol^{-1}$. The plate was covered and incubated
733 at RT for 3 h on a horizontal orbital plate shaker. Following incubation, plate contents
734 were discarded, and wells were washed four times with 200 µL/well of 1X wash buffer.
735 Next, 100 µL of 3,3',5,5'-tetramethylbenzidine (TMB) substrate was added to each well,
736 and the plate was covered and kept for 10 min at RT. The enzymatic reaction was

737 quenched by adding 100 µL of 2 $mmol^{-1}$ HCl and absorbance read at 450 nm using a
738 Synergy 2 Microplate Reader (Biotek).
739
740 **Statistical analyses**
741 Data was compiled using Microsoft Excel and transferred to Graphpad Prism
742 software v.7 to create figures and conduct all statistical analyses. Data was analyzed
743 accordingly using a one-way or two-way ANOVA and a Bonferroni post-test, or
744 Student's t-test, with differences between treatments considered significant if $p<0.05$.
745
746 **Acknowledgments**
747 The authors sincerely thank Prof. Helmut Wieczorek and Prof. Felix Tiburcy (University
748 of Osnabrück, Germany) for providing the V_1 antibody and Prof. Andrew Donini (York
749 University, Canada) for providing the *A. aegypti* AQP1 antibody that were used in this
750 study. The authors are also grateful to Prof. Ian Orchard (University of Toronto
751 Mississauga, Canada) and Prof. Michael J. O'Donnell (McMaster University, Canada) for
752 providing synthetic peptides, *Rhopr*DH and *Drome*DH_{31} respectively, used in this study.
753
754 **Funding**
755 This research was funded by: Natural Sciences and Engineering Research Council of
756 Canada (NSERC) Discovery Grant (JPP)**,** Ontario Ministry of Research Innovation Early
757 Researcher Award (JPP), and NSERC CGS-D (FS) and the Carswell Scholarships in the
758 Faculty of Science, York University (FS) along with a MITACS Globalink Research
759 Internship (MFV).

760

761 **Data and materials availability**

762 All data are available in the main text or the supplementary materials. Additional data

763 related to this paper may be requested from the authors.

764

765 **Figures and Tables**

766 **Fig. 1.** Effect of bafilomycin on fluid secretion rates and pH along with cyclic nucleotide

767 second messengers on adult *A. aegypti* MTs. Tubules were treated with either (A) DH_{31}

768 (B) 5HT or (C) DH_{44} and secreted droplets were measured at 10-min intervals for 30 min.

769 Immediately following measurement of the 30-min point fluid droplet (solid arrow), MTs

770 were treated with (A) DH_{31} (B) 5HT (C) or DH_{44} alone or in combination with

771 *Aedae*CAPA-1 or bafilomycin. (D) MTs were treated with DH_{31} alone or in combination

772 with *Aedae*CAPA-1, bafilomycin, or both *Aedae*CAPA-1 and bafilomycin for 60 min.

773 Secreted fluid pH was measured in tubules treated with either (E) DH_{31} (F) 5HT or (G)

774 DH_{44} before and after addition of *Aedae*CAPA-1, bafilomycin, or both *Aedae*CAPA-1

775 and bafilomycin along with unstimulated MTs (H). Production of (I) cGMP and (J)

776 cAMP in DH_{31}-stimulated MTs treated with *Aedae*CAPA-1. (A-C) Significant

777 differences between bafilomycin-treated and the corresponding time point controls and

778 (E-H) significant differences in secreted fluid pH between *Aedae*CAPA-1- and

779 bafilomycin-treated and the corresponding time point controls are denoted by an asterisk,

780 as determined by a two-way ANOVA and Bonferroni multiple comparison post-hoc test

781 ($p<0.05$). Data represent the mean ± standard error (n=12-34), ns denotes no statistical

782 significance. (D, I, J) Bars labeled with different letters are significantly different from

783 each other (mean± SEM; one-way ANOVA with Bonferroni multiple comparison,
784 $p<0.05$, (D) n=7-17) (I, J) n=50 sets of MTs for all treatments (n=3 per treatment)). (K)
785 Fluid secretion rates were measured at 10 min intervals initially over a 30 min interval
786 (unstimulated) and then over a second 30 min interval after the addition (solid arrow) of
787 10^{-4} M cAMP or 10^{-8} M cGMP. Significant differences between cAMP-treated MTs and
788 the corresponding time point controls (or cGMP- treated MTs) are denoted by an asterisk
789 (mean± SEM; two-way ANOVA with Bonferroni multiple comparison, $p<0.05$, n=5-6).
790 (L) Significant differences between cAMP-treated MTs and corresponding time point
791 after addition at 30 min (downward arrow) of cGMP are denoted by an asterisk (similar
792 with cGMP alone and cAMP added at 30 min, mean± SEM; one-way ANOVA with
793 Bonferroni multiple comparison, $p<0.05$, n=5-9).
794
795 **Fig. 2.** Effect of *Aedae*CAPA-1 and NOS/PKG inhibitors on VA and NKA activity in
796 diuretic stimulated *A. aegypti* MTs. MTs were incubated in *Aedes* saline, diuretics (DH_{31},
797 5HT, and DH_{44}) alone or in combination with *Aedae*CAPA-1 for 30 min before collection
798 to measure (A) VA and (B) NKA activity. (C) MTs were treated with pharmacological
799 blockers, NOS inhibitor ($_L$-NAME) and PKG inhibitor (KT5923) in combination with
800 either *Aedae*CAPA-1 or cGMP. Bars labeled with different letters are significantly
801 different from each other (mean± SEM; one-way ANOVA with Bonferroni multiple
802 comparison, $p<0.05$). N.S. denotes no statistical significance. For each treatment, 50 sets
803 of MTs were collected with n=3 biological replicates per treatment.
804

Fig. 3. Membrane and cytosolic protein abundance of the V_1 complex in MTs of *A. aegypti*. The MTs (n=40-50) were incubated in *Aedes* saline, DH_{31}, or DH_{31} + *Aedae*CAPA-1 for one hour before collection. Protein abundance was measured in the (A) 74 kDa band, A subunit (B) 56 kDa band, B subunit and (c) 32 kDa band, D subunit of the V_1 complex. Individual band densities were normalized to total protein using Coomassie staining, and graphed relative to saline-treated controls. Bars labeled with different letters are significantly different from each other (mean± SEM; one-way ANOVA with Bonferroni multiple comparison, $p<0.05$, n=3-4 replicates).

Fig. 4. Immunolocalization of the V_o and V_1 complexes in transverse sections of stimulated *A. aegypti* MTs. Representative paraffin-embedded sections of *A. aegypti* MTs incubated in either (A-C) *Aedes* saline alone, (D-F) DH_{31} and (G-I) DH_{31} + *Aedae*CAPA-1 for 30 min. Panels (A,D,G) show V_o staining (red), (B,E,H) show V_1 staining (green), and panels (C,F,I) show merged images with staining highly colocalized in DH_{31} treatment but less evident in saline and *Aedae*CAPA-1 added treatments. Solid white arrows denote apical VA staining, and empty arrows indicate cytosolic VA staining. Where visible in sections, DAPI nuclear staining is shown in blue. Scale bar 100 µm, n = 4 biological replicates (SC = stellate cell).

Fig. 5. Immunolocalization of the V_o and V_1 complexes in blood-fed *A. aegypti* females. Representative paraffin-embedded sections of whole-body non-blood-fed females (A-C), blood-fed females isolated (D-F) 10 min (G-I) 30 min and (J-L) 3 hr post blood-meal. Panels (A,D,G,J) show V_o staining (red), (B,E,H,K) show V_1 staining (green), and panels

(C,F,I,L) show merged immunoreactive staining. DAPI nuclear staining is shown in blue. Scale bar 100 μm, n = 4 biological replicates.

Fig. 6. Schematic diagram summarizing the signaling pathway of diuretic and anti-diuretic control of adult *A. aegypti* MTs. The principal cells in *A. aegypti* MTs are responsible for the transport of Na^+ and K^+ cations via secondary active transport, energized by the V-type H^+-ATPase (VA), localized in the brush border of the apical membrane. The movement of protons creates a gradient, driving the exchange of Na^+ and K^+ through cation/H^+ antiporters (NHA). Neurohormone receptors for DH_{31}, 5HT, DH_{44}, and CAPA are localized to the basolateral membrane of the principal cells, while the kinin receptor is localized exclusively in the stellate cells. The current results together with previous data indicates that DH_{31} stimulates diuresis through activation and assembly of the VA in the apical membrane, with no effect on the Na^+/K^+-ATPase (NKA). The anti-diuretic effect of *Aedae*CAPA-1, facilitated by the NOS/cGMP/PKG pathway, causes V_1 dissociation from the membrane, hindering activity, and thus reducing fluid secretion. The biogenic amine, 5HT, has also been shown to stimulate activation of the VA, however, to a lesser extent. DH_{44}-related peptide receptor activation increases Ca^{2+} (as well as cAMP at higher doses) but its action was found to be independent of PKA and VA. Lastly, it was shown earlier that cGMP inhibits kinin-stimulated diuresis, suggesting an additional anti-diuretic factor may exist that acts specifically on stellate cells.

References

1. K. W. Beyenbach, Transport mechanisms of diuresis in Malpighian tubules of insects. *J. Exp. Biol.* **206**, 3845–3856 (2003).

2. T. M. Clark, T. J. Bradley, Malpighian tubules of larval *Aedes aegypti* are hormonally stimulated by 5-hydroxytryptamine in response to increased salinity. *Arch. Insect Biochem. Physiol.* **34**, 123–141 (1997).

3. G. M. Coast, C. S. Garside, Neuropeptide control of fluid balance in insects, *Ann. N.Y. Acad. Sci.* **1040**: 1–8 (2005).

4. F. Sajadi, C. Curcuruto, A. Al Dhaheri, J.-P. V Paluzzi, Anti-diuretic action of a CAPA neuropeptide against a subset of diuretic hormones in the disease vector, *Aedes aegypti*. *J. Exp. Biol.* (2018).

5. H. L. Lu, C. Kersch, P. V. Pietrantonio, The kinin receptor is expressed in the Malpighian tubule stellate cells in the mosquito *Aedes aegypti* (L.): A new model needed to explain ion transport? *Insect Biochem. Mol. Biol.* **41**, 135–140 (2011).

6. F. Sajadi, *et al.*, CAPA neuropeptides and their receptor form an anti-diuretic hormone signaling system in the human disease vector, *Aedes aegypti*. *Sci. Rep.* **10** (2020).

7. A. Ionescu, A. Donini, *Aedes*CAPA-PVK-1 displays diuretic and dose dependent antidiuretic potential in the larval mosquito *Aedes aegypti* (Liverpool). *J. Insect Physiol.* **58**, 1299–1306 (2012).

8. R. Jurenka, The PRXamide neuropeptide signalling system. Conserved in animals,

Adv. Insect Phys. (Academic Press, 2015), pp. 123–170.

9. S. A. Davies, *et al.*, Signaling by *Drosophila* capa neuropeptides. *Gen. Comp. Endocrinol.* **188**, 60–66 (2012).

10. S. Terhzaz, *et al.*, Mechanism and function of *drosophila* capa GPCR: A desiccation stress-responsive receptor with functional homology to human neuromedinu receptor. *PLoS One* **7** (2012).

11. H. A. MacMillan, *et al.*, Anti-diuretic activity of a CAPA neuropeptide can compromise *Drosophila* chill tolerance. *J. Exp. Biol.* **221**, jeb185884 (2018).

12. A. R. Rodan, M. Baum, C. L. Huang, The *drosophila* NKCC Ncc69 is required for normal renal tubule function. *Am. J. Physiol. - Cell Physiol.* **303**, C883–C894 (2012).

13. X. H. Weng, M. Huss, H. Wieczorek, K. W. Beyenbach, The V-type H^+-ATPase in Malpighian tubules of *Aedes aegypti*: localization and activity. *J. Exp. Biol.* **206**, 2211–2219 (2003).

14. H. Wieczorek, K. W. Beyenbach, M. Huss, O. Vitavska, Vacuolar-type proton pumps in insect epithelia. *J. Exp. Biol.* **212**, 1611–1619 (2009).

15. H. Wieczorek, The insect V-ATPase, a plasma membrane proton pump energizing secondary active transport: molecular analysis of electrogenic potassium transport in the tobacco hornworm midgut. *J. Exp. Biol.* **172**, 335–343 (1992).

16. H. Wieczorek, M. Putzenlechnere, U. Klein, A Vacuolar-type proton pump energizes K^+/H^+ antiport in an animal plasma membrane. *J. Biol. Chem.* **266**,

15340–15347 (1991).

17. W. R. Harvey, S. H. P. Maddrell, W. H. Telfer, H. Wieczorek, H^+ V-ATPases energize animal plasma membranes for secretion and absorption of ions and fluids. *Am. Zool.* **38**, 426–441 (1998).

18. Y. Li, *et al.*, RNA-Seq comparison of larval and adult malpighian tubules of the yellow fever mosquito *Aedes aegypti* reveals life stage-specific changes in renal function. *Front. Physiol.* **8**, 1–13 (2017).

19. M. L. Patrick, K. Aimanova, H. R. Sanders, S. S. Gill, P-type Na^+/K^+-ATPase and V-type H^+-ATPase expression patterns in the osmoregulatory organs of larval and adult mosquito *Aedes aegypti*. *J. Exp. Biol.* **209**, 4638–4651 (2006).

20. K. W. Beyenbach, T. L. Pannabecker, W. Nagel, Central role of the apical membrane H^+-ATPase in electrogenesis and epithelial transport in Malpighian tubules. *J. Exp. Biol.* **203**, 1459–1468 (2000).

21. R. M. Hine, *et al.*, The excretion of NaCl and KCl loads in mosquitoes. *Am. J. Physiol. - Regul. Integr. Comp. Physiol.* **307**, R837–R849 (2014).

22. P. Dames, *et al.*, cAMP regulates plasma membrane vacuolar-type H^+-ATPase assembly and activity in blowfly salivary glands. *Proc. Natl. Acad. Sci. U. S. A.* **103**, 3926–3931 (2006).

23. G. M. Coast, C. S. Garside, S. G. Webster, K. M. Schegg, D. A. Schooley, Mosquito natriuretic peptide identified as a calcitonin-like diuretic hormone in *Anopheles gambiae* (Giles). *J. Exp. Biol.* **208**, 3281–3291 (2005).

913 24. K. Karas, P. Brauer, D. Petzel, Actin redistribution in mosquito Malpighian
914 tubules after a blood meal and cyclic AMP stimulation. *J. Insect Physiol.* **51**,
915 1041–1054 (2005).

916 25. C. Cady, H. H. Hagedorn, Effects of putative diuretic factors on intracellular
917 second messenger levels in the Malpighian tubules of *Aedes aegypti*. *J. Insect*
918 *Physiol.* **45**, 327–337 (1999).

919 26. D. H. Petzel, P. T. Pirotte, E. Van Kerkhove, Intracellular and luminal pH
920 measurements of malpighian tubules of the mosquito *Aedes aegypti*: the effects of
921 cAMP. *J. Insect Physiol.* **45**, 973–982 (1999).

922 27. T. M. Clark, T. K. Hayes, K. W. Beyenbach, Dose-dependent effects of CRF-like
923 diuretic peptide on transcellular and paracellular transport pathways. *Am. J.*
924 *Physiol. - Ren. Physiol.* **274** (1998).

925 28. K. W. Beyenbach, H. Wieczorek, The V-type H^+ ATPase: molecular structure and
926 function, physiological roles and regulation. *J. Exp. Biol.* **209**, 577–589 (2006).

927 29. F. J. S. Novak, *et al.*, Primary structure of V-ATPase subunit B from *Manduca*
928 *sexta midgut*. *BBA - Gene Struct. Expr.* **1132**, 67–71 (1992).

929 30. Y. X. Pan, H. H. Gu, J. Xu, G. E. Dean, *Saccharomyces cerevisiae* expression of
930 exogenous vacuolar ATPase subunits B. *BBA - Biomembr.* **1151**, 175–185 (1993).

931 31. H. Wieczorek, D. Brown, S. Grinstein, J. Ehrenfeld, W. R. Harvey, Animal plasma
932 membrane energization by proton-motive V-ATPases. *BioEssays* **21**, 637–648
933 (1999).

934 32. J. Zhang, Y. Feng, M. Forgac, Proton conduction and bafilomycin binding by the
935 V0 domain of the coated vesicle V-ATPase. *J. Biol. Chem.* **269**, 23518–23523
936 (1994).

937 33. W. J. A. Dschida, B. J. Bowman, The vacuolar ATPase: sulfite stabilization and
938 the mechanism of nitrate inactivation. *J. Biol. Chem.* **270**, 1557–1563 (1995).

939 34. J. Rein, M. Voss, W. Blenau, B. Walz, O. Baumann, Hormone-induced assembly
940 and activation of V-ATPase in blowfly salivary glands is mediated by protein
941 kinase A. *Am. J. Physiol. - Cell Physiol.* **294**, C56–C65 (2008).

942 35. B. Zimmermann, P. Dames, B. Walz, O. Baumann, Distribution and serotonin-
943 induced activation of vacuolar-type H^+-ATPase in the salivary glands of the
944 blowfly *Calliphora vicina*. *J. Exp. Biol.* **206**, 1867–1876 (2003).

945 36. H. Wieczorek, G. Grüber, W. R. Harvey, M. Huss, H. Merzendorfer, The plasma
946 membrane H^+-V-ATPase from tobacco hornworm midgut. *J. Bioenerg. Biomembr.*
947 **31**, 67–74 (1999).

948 37. M. C. Quinlan, N. J. Tublitz, M. J. O'Donnell, Anti-diuresis in the blood-feeding
949 insect *Rhodnius prolixus* Stal: The peptide CAP(2b) and cyclic GMP inhibit
950 Malpighian tubule fluid secretion. *J. Exp. Biol.* **200**, 2363–2367 (1997).

951 38. F. Tiburcy, K. W. Beyenbach, H. Wieczorek, Protein kinase A-dependent and -
952 independent activation of the V-ATPase in Malpighian tubules of *Aedes aegypti*. *J.*
953 *Exp. Biol.* **216**, 881–891 (2013).

954 39. K. W. Beyenbach, P. M. Piermarini, Transcellular and paracellular pathways of

transepithelial fluid secretion in Malpighian (renal) tubules of the yellow fever mosquito *Aedes aegypti*. *Acta Physiol. (Oxf).* **202**, 387–407 (2011).

40. K. W. Beyenbach, Energizing epithelial transport with the vacuolar H^+-ATPase. *News Physiol. Sci.* **16**, 145–151 (2001).

41. T. Nishi, M. Forgac, The vacuolar (H^+)-ATPases - nature's most versatile proton pumps. *Nat. Rev. Mol. Cell Biol.* **3**, 94–103 (2002).

42. N. Nelson, W. R. Harvey, Vacuolar and plasma membrane proton-adenosinetriphosphatases. *Physiol. Rev.* **79**, 361–385 (1999).

43. K. W. Beyenbach, H. Skaer, J. A. T. Dow, The developmental, molecular, and transport biology of malpighian tubules. *Annu. Rev. Entomol.* **55**, 351–374 (2010).

44. P. M. Kane, Disassembly and reassembly of the yeast vacuolar H^+-ATPase in vivo. *J. Biol. Chem.* **270**, 17025–17032 (1995).

45. M. Voss, O. Vitavska, B. Walz, H. Wieczorek, O. Baumann, Stimulus-induced phosphorylation of vacuolar H^+-ATPase by protein kinase A. *J. Biol. Chem.* **282**, 33735–33742 (2007).

46. J. P. Sumner, *et al.*, Regulation of plasma membrane V-ATPase activity by dissociation of peripheral subunits. *J. Biol. Chem.* **270**, 5649–5653 (1995).

47. G. Coast, The endocrine control of salt balance in insects. *Gen. Comp. Endocrinol.* **152**, 332–338 (2007).

48. M. J. O'Donnell, J. H. Spring, Modes of control of insect Malpighian tubules:

synergism, antagonism, cooperation and autonomous regulation. *J. Insect Physiol.* **46**, 107–117 (2000).

49. J. C. Williams, H. H. Hagedorn, K. W. Beyenbach, Dynamic changes in flow rate and composition of urine during the post-bloodmeal diuresis in *Aedes aegypti* (L.). *J. Comp. Physiol.* **153**, 257–265 (1983).

50. C. L. Jagge, P. V. Pietrantonio, Diuretic hormone 44 receptor in Malpighian tubules of the mosquito *Aedes aegypti*: evidence for transcriptional regulation paralleling urination. *Insect Mol. Biol.* **17**, 413–426 (2008).

51. P. Gioino, B. G. Murray, J. P. Ianowski, Serotonin triggers cAMP and PKA-mediated intracellular calcium waves in Malpighian tubules of *Rhodnius prolixus*. *Am. J. Physiol. - Regul. Integr. Comp. Physiol.* **307**, R828–R836 (2014).

52. F. Sajadi, J. P. V. Paluzzi, Hormonal regulation and functional role of the 'renal' tubules in the disease vector, *Aedes aegypti*. *Vitamins and Hormones*, (Academic Press, 2021), pp. 189–225.

53. P. V. Pietrantonio, C. Jagge, C. McDowell, Cloning and expression analysis of a 5HT7-like serotonin receptor cDNA from mosquito *Aedes aegypti f*emale excretory and respiratory systems. *Insect Mol. Biol.* **10**, 357–369 (2001).

54. D. W. Lee, P. V. Pietrantonio, In vitro expression and pharmacology of the 5-HT7-like receptor present in the mosquito *Aedes aegypti* tracheolar cells and hindgut-associated nerves. *Insect Mol. Biol.* **12**, 561–569 (2003).

55. A. Petrova, D. F. Moffett, Comprehensive immunolocalization studies of a

putative serotonin receptor from the alimentary canal of *Aedes aegypti* larvae suggest its diverse roles in digestion and homeostasis. *PLoS One* **11**, e0146587 (2016).

56. K. . Clark, T M, Hayes, T K., Holman, G.M., Beyenbach, The concentration-dependence of CRF-like diuretic peptide: mechanisms of action. *J. Exp. Biol.* **201**, 1753–1762 (1998).

57. D. H. Petzel, H. H. Hagedorn, K. W. Beyenbach, Preliminary isolation of mosquito natriuretic factor. *Am. J. Physiol. - Regul. Integr. Comp. Physiol.* **18** (1985).

58. J. A. Dow, *et al.*, The malpighian tubules of *Drosophila melanogaster*: a novel phenotype for studies of fluid secretion and its control. *J. Exp. Biol.* **197**, 421–428 (1994).

59. D. H. Petzel, M. M. Berg, K. W. Beyenbach, Hormone-controlled cAMP-mediated fluid secretion in yellow-fever mosquito. *Am. J. Physiol. - Regul. Integr. Comp. Physiol.* **253** (1987).

60. H. Kwon, H. L. Lu, M. T. Longnecker, P. V. Pietrantonio, Role in diuresis of a calcitonin receptor (GPRCAL1) expressed in a distal-proximal gradient in renal organs of the mosquito *Aedes aegypti* (L.). *PLoS One* **7**, e50374 (2012).

61. W. Kang'ethe, K. G. Aimanova, A. K. Pullikuth, S. S. Gill, NHE8 mediates amiloride-sensitive Na^+/H^+ exchange across mosquito Malpighian tubules and catalyzes Na^+ and K^+ transport in reconstituted proteoliposomes. *Am. J. Physiol. -*

Ren. Physiol. **292**, 1501–1512 (2007).

62. A. K. Pullikuth, K. Aimanova, W. Kang'ethe, H. R. Sanders, S. S. Gill, Molecular characterization of sodium/proton exchanger 3 (NHE3) from the yellow fever vector, *Aedes aegypti*. *J. Exp. Biol.* **209**, 3529–3544 (2006).

63. P. M. Piermarini, D. Weihrauch, H. Meyer, M. Huss, K. W. Beyenbach, NHE8 is an intracellular cation/H^+ exchanger in renal tubules of the yellow fever mosquito *Aedes aegypti*. *Am. J. Physiol. - Ren. Physiol.* **296**, 730–750 (2009).

64. H. Merzendorfer, M. Huss, R. Schmid, W. R. Harvey, H. Wieczorek, A novel insect V-ATPase subunit M9.7 is glycosylated extensively. *J. Biol. Chem.* **274**, 17372–17378 (1999).

65. M. C. Quinlan, M. J. O'Donnell, Anti-diuresis in the blood-feeding insect *Rhodnius prolixus* Stal: antagonistic actions of cAMP and cGMP and the role of organic acid transport. *J. Insect Physiol.* **44**, 561–568 (1998).

66. S. Seino, T. Shibasaki, PKA-dependent and PKA-independent pathways for cAMP-regulated exocytosis. *Physiol. Rev.* **85**, 1303–1342 (2005).

67. M. Efetova, *et al.*, Separate roles of PKA and EPAC in renal function unraveled by the optogenetic control of cAMP levels in vivo. *J. Cell Sci.* **126**, 778–788 (2013).

68. K. W. Beyenbach, A. Oviedo, D. J. Aneshansley, Malpighian tubules of *Aedes aegypti*: five tubules, one function. *J. Insect Physiol.* **39**, 639–648 (1993).

69. J. A. Veenstra, Effects of 5-hydroxytryptamine on the Malpighian tubules of *Aedes aegypti*. *J. Insect Physiol.* **34**, 299–304 (1988).

1038 70. J. P. V. Paluzzi, W. Naikkhwah, M. J. O'Donnell, Natriuresis and diuretic
1039 hormone synergism in *R. prolixus* upper Malpighian tubules is inhibited by the
1040 anti-diuretic hormone, *Rhopr*CAPA-α2. *J. Insect Physiol.* **58**, 534–542 (2012).

1041 71. D. A. Rocco, D. H. Kim, J. P. V. Paluzzi, Immunohistochemical mapping and
1042 transcript expression of the GPA2/GPB5 receptor in tissues of the adult mosquito,
1043 *Aedes aegypti*. *Cell Tissue Res.* **369**, 313–330 (2017).

1044 72. A. Lajevardi, F. Sajadi, A. Donini, J. P. V. Paluzzi, Studying the activity of
1045 neuropeptides and other regulators of the excretory system in the adult mosquito.
1046 *J. Vis. Exp.* **2021** (2021).

1047 73. M. Vanderveken, M. J. O'Donnell, Effects of diuretic hormone 31, *droso*kinin, and
1048 allatostatin A on transepithelial K^+ transport and contraction frequency in the
1049 midgut and hindgut of larval *Drosophila melanogaster*. *Arch. Insect Biochem.*
1050 *Physiol.* **85**, 76–93 (2014).

1051 74. T. M. Clark, T. J. Bradley, Additive effects of 5-HT and diuretic peptide on *Aedes*
1052 malpighian tubule fluid secretion. *Comp. Biochem. Physiol. - A Mol. Integr.*
1053 *Physiol.* **119**, 599–605 (1998).

1054 75. V. Te Brugge, J. P. Paluzzi, D. A. Schooley, I. Orchard, Identification of the
1055 elusive peptidergic diuretic hormone in the blood-feeding bug *Rhodnius prolixus*: a
1056 CRF-related peptide. *J. Exp. Biol.* **214**, 371–381 (2011).

1057 76. H. R. Lee, M. Zandawala, A. B. Lange, I. Orchard, Isolation and characterization
1058 of the corticotropin-releasing factor-related diuretic hormone receptor in *Rhodnius*

prolixus. *Cell. Signal.* **28**, 1152–1162 (2016).

77. M. R. Rheault, M. J. O'Donnell, Organic cation transport by Malpighian tubules of *Drosophila melanogaster*: application of two novel electrophysiological methods. *J. Exp. Biol.* **207**, 2173–2184 (2004).

78. S. Jonusaite, S. P. Kelly, A. Donini, The physiological response of larval *Chironomus riparius* (Meigen) to abrupt brackish water exposure. *J. Comp. Physiol. B Biochem. Syst. Environ. Physiol.* **181**, 343–352 (2011).

79. S. D. McCormick, Methods for nonlethal gill biopsy and measurement of Na^+, K^+-ATPase activity. *Can. J. Fish. Aquat. Sci.* **50**, 656–658 (1993).

80. A. J. Fosang, R. J. Colbran, Transparency is the key to quality. *J. Biol. Chem.* **290**, 29692–29694 (2015).

81. T. A. J. Butler, J. W. Paul, E. C. Chan, R. Smith, J. M. Tolosa, Misleading westerns: common quantification mistakes in western blot densitometry and proposed corrective measures. *Biomed Res. Int.* **2019** (2019).

82. A. C. Durant, A. Donini, Ammonium transporter expression in sperm of the disease vector *Aedes aegypti* mosquito influences male fertility. *Proc. Natl. Acad. Sci. U. S. A.* **117**, 29712–29719 (2020).

83. L. Misyura, E. G. Guardian, A. C. Durant, A. Donini, A comparison of aquaporin expression in mosquito larvae (*Aedes aegypti*) that develop in hypo-osmotic freshwater and iso-osmotic brackish water. *PLoS One* **15**, e0234892 (2020).

84. H. Chasiotis, S. P. Kelly, Occludin immunolocalization and protein expression in

goldfish. *J. Exp. Biol.* **211**, 1524–1534 (2008).

85. L. Kean, *et al.*, Two nitridergic peptides are encoded by the gene capability in *Drosophila melanogaster*. *Am. J. Physiol. - Regul. Integr. Comp. Physiol.* **282** (2002).

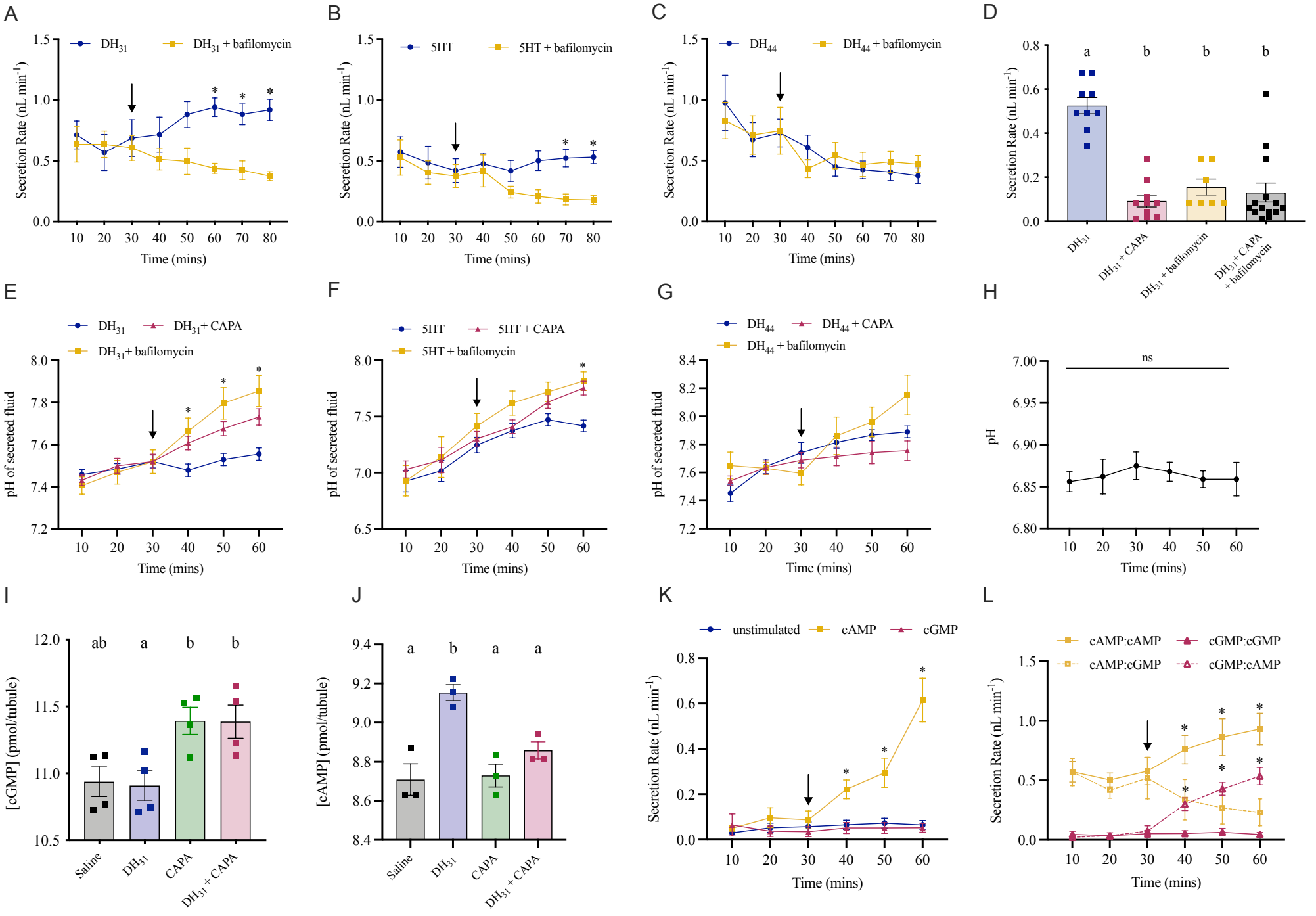
A
DH31
DH31 + bafilomycin
Secretion Rate (nL min-1)
Time (mins)
B
5HT
5HT + bafilomycin
C
DH44
DH44 + bafilomycin
D
a
b
b
b
DH31
DH31 + CAPA
DH31 + bafilomycin
DH31 + CAPA + bafilomycin
E
DH31
DH31+ CAPA
DH31+ bafilomycin
pH of secreted fluid
F
5HT
5HT + CAPA
5HT + bafilomycin
G
DH44
DH44 + CAPA
DH44 + bafilomycin
H
ns
pH
I
ab
a
b
b
[cGMP] (pmol/tubule)
Saline
DH31
CAPA
DH31 + CAPA
J
a
b
a
a
[cAMP] (pmol/tubule)
K
unstimulated
cAMP
cGMP
L
cAMP:cAMP
cGMP:cGMP
cAMP:cGMP
cGMP:cAMP

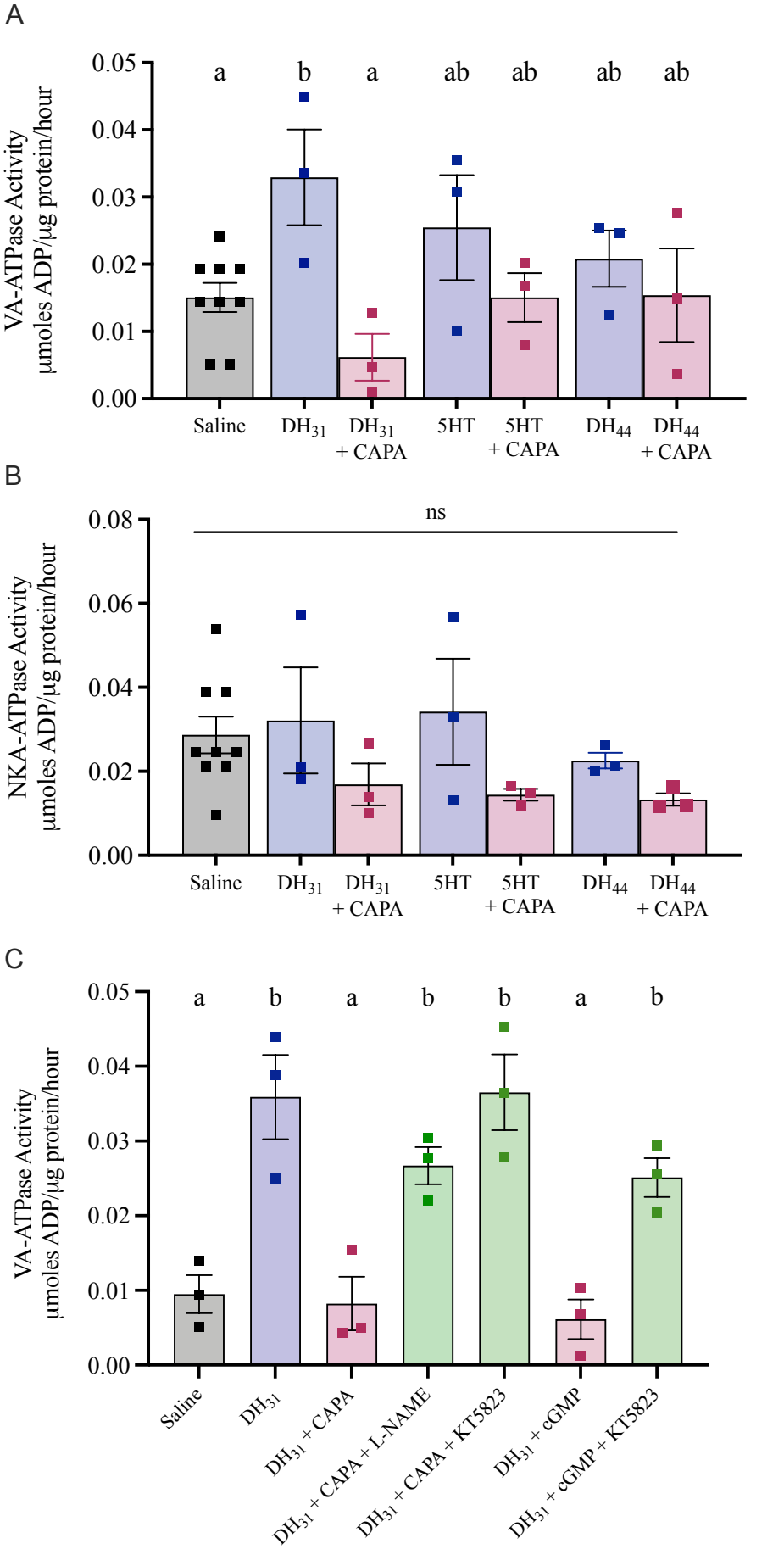
A
VA-ATPase Activity
µmoles ADP/µg protein/hour
0.05
0.04
0.03
0.02
0.01
0.00
a
b
a
ab
ab
ab
ab
Saline
DH31
DH31 + CAPA
5HT
5HT + CAPA
DH44
DH44 + CAPA
B
NKA-ATPase Activity
µmoles ADP/µg protein/hour
0.08
0.06
0.04
0.02
0.00
ns
Saline
DH31
DH31 + CAPA
5HT
5HT + CAPA
DH44
DH44 + CAPA
C
VA-ATPase Activity
µmoles ADP/µg protein/hour
0.05
0.04
0.03
0.02
0.01
0.00
a
b
a
b
b
a
b
Saline
DH31
DH31 + CAPA
DH31 + CAPA + L-NAME
DH31 + CAPA + KT5823
DH31 + cGMP
DH31 + cGMP + KT5823

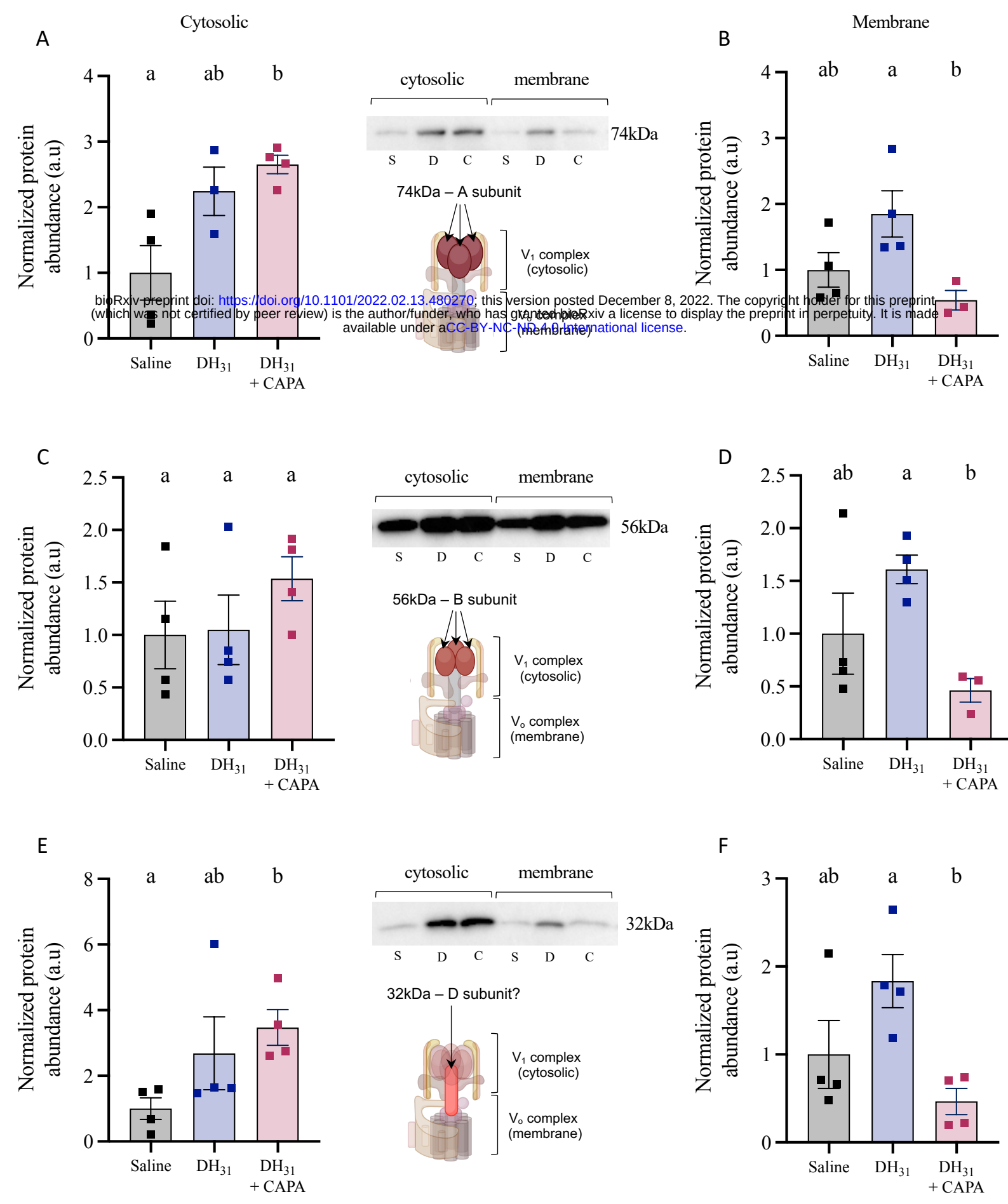

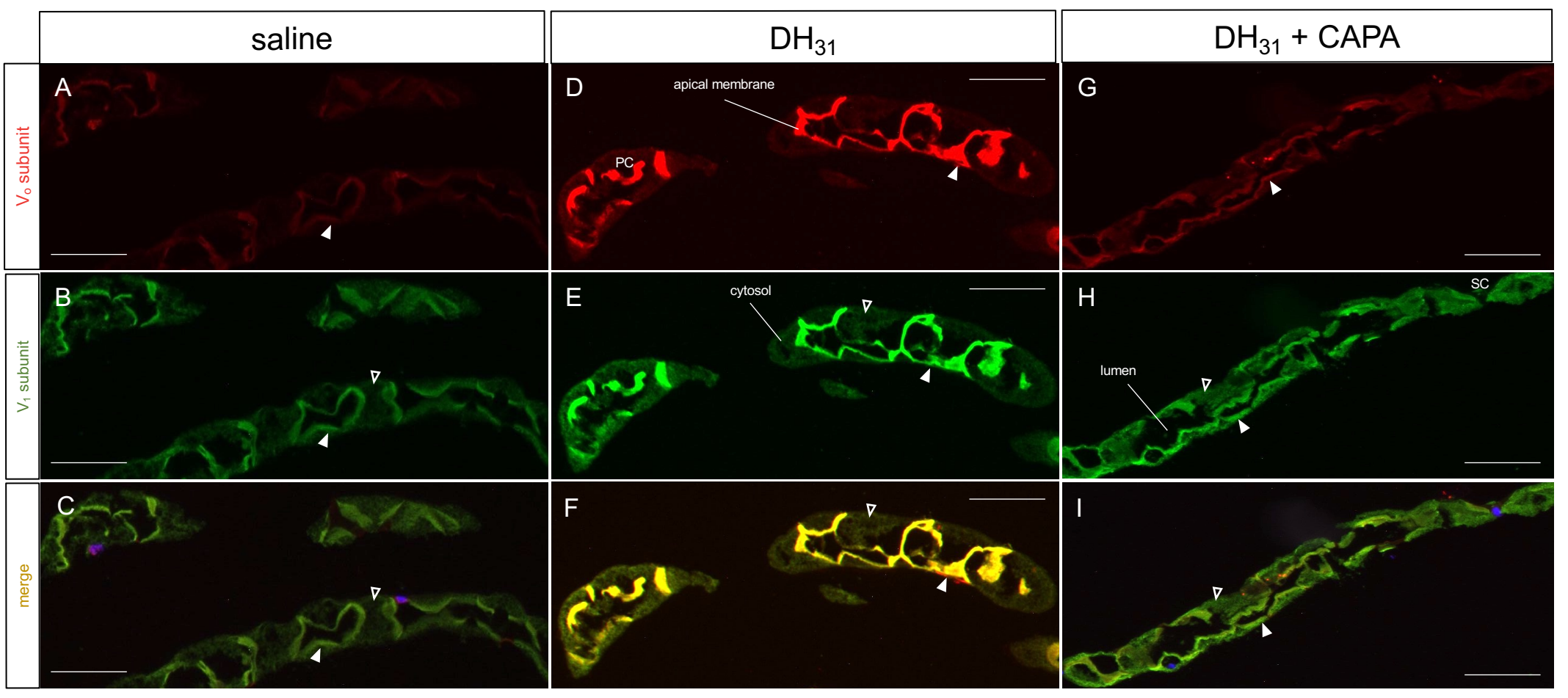
saline
DH31
DH31 + CAPA
Vo subunit
V1 subunit
merge
A
B
C
D
E
F
G
H
I
apical membrane
PC
cytosol
lumen
SC

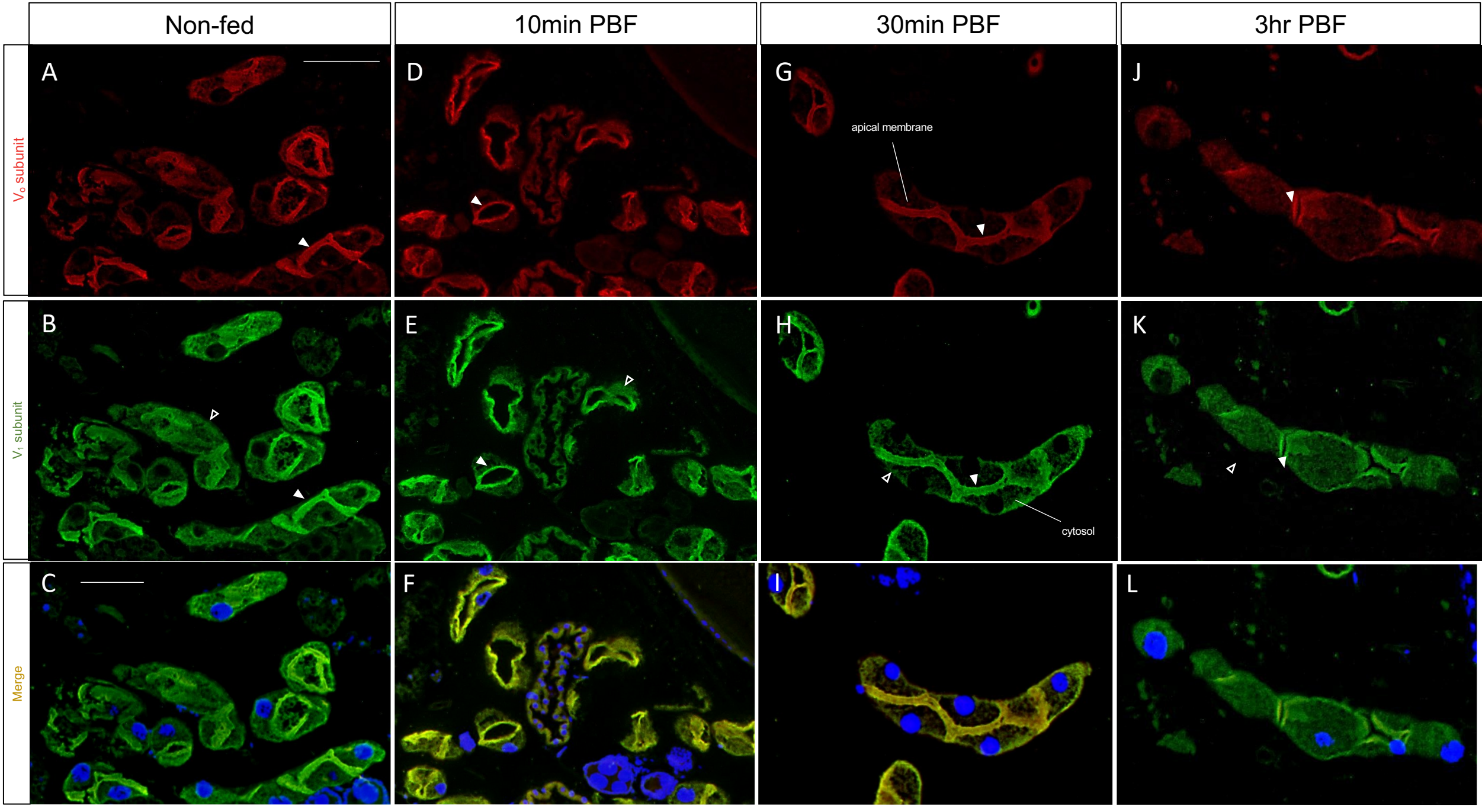
Non-fed
10min PBF
30min PBF
3hr PBF
V_o subunit
V_1 subunit
Merge
A
B
C
D
E
F
G
H
I
J
K
L
apical membrane
cytosol

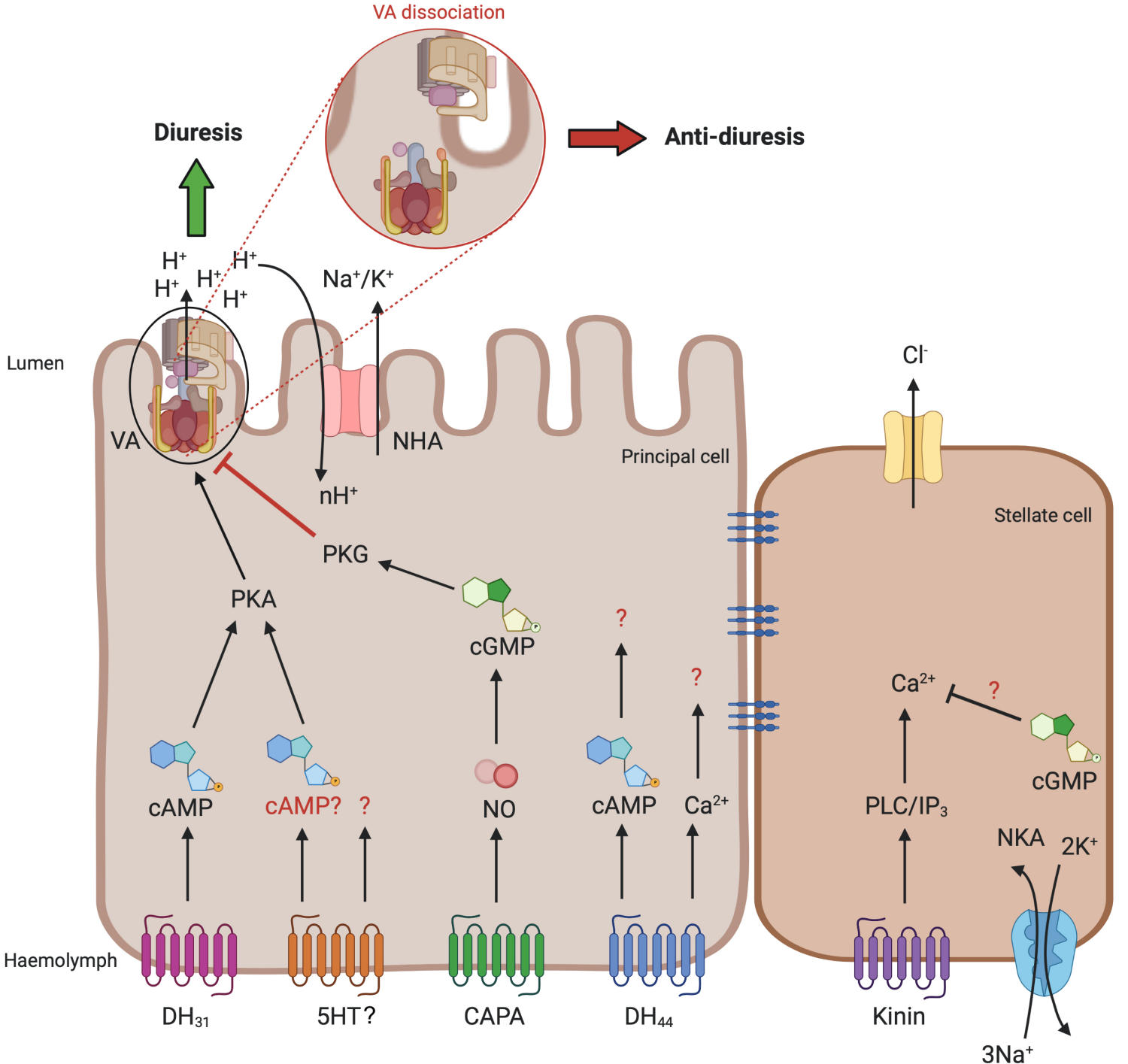
VA dissociation
Diuresis
Anti-diuresis
H+
H+
H+
H+
H+
Na+/K+
Lumen
VA
NHA
nH+
Principal cell
Cl-
Stellate cell
PKG
PKA
cGMP
?
?
Ca2+
?
cAMP
cAMP?
?
NO
cAMP
Ca2+
PLC/IP3
cGMP
NKA
2K+
Haemolymph
DH31
5HT?
CAPA
DH44
Kinin
3Na+